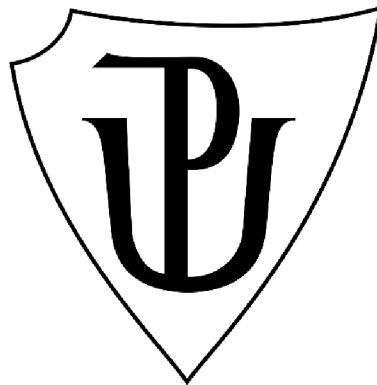# UNIVERZITA PALACKÉHO V OLOMOUCI

Prírodovedecká fakulta

Katedra biotechnológií

Tvorba reaktívnych foriem kyslíku v kožných bunkách

BAKALÁRSKA PRÁCA

Autor:	**Hana Duchová**
Študijný program:	B0512A130007 Biotechnológie a génové inžinierstvo
Špecializácia:	Biotechnológie a génové inžinierstvo
Forma štúdia:	Prezenčná
Vedúci práce:	**doc. Ankush Prasad, Ph.D.**
Rok:	2023

PALACKY UNIVERSITY IN OLOMOUC

Faculty of Science

Department of Biotechnology

Formation of reactive oxygen species in skin cells

BACHELOR THESIS

Author:	**Hana Duchová**
Study Program:	B0512A130007 Biotechnology and Gene Engineering
Specialty:	Biotechnology and Gene Engineering
Form:	Full-time
Supervisor:	**doc. Ankush Prasad, Ph.D.**
Year:	2023

Prehlasujem, že bakalársku prácu som vypracovala samostatne s vyznačením všetkých použitých prameňov a spoluautorstiev. Súhlasím so zverejnením bakalárskej práce podľa zákona č. 111/1998 Sb., o vysokých školách, v znení neskorších predpisov. Bola som oboznámená s tým, že sa na moju prácu vzťahujú práva a povinnosti vyplývajúce zo zákona č. 121/2000 Sb., autorský zákon, v znení neskorších predpisov.

V Olomouci dňa ....
                                                                        Podpis študenta

Bibliografická identifikácia

Meno a priezvisko autora	Hana Duchová
Názov práce	Tvorba reaktívnych kyslíkových radikálov v kožných bunkách
Typ práce	Bakalárska
Pracovisko	Katedra biofyziky
Vedúci práce	doc. Ankush Prasad, Ph.D.
Rok obhajoby práce	2023

Abstrakt

Koža zohráva kľúčovú úlohu v mnohých rozličných telesných funkciách/procesoch vrátane metabolizmu, ochrany, termoregulácie, vylučovania a vnímania. A to aj napriek jej neustálemu vystaveniu biotickým aj abiotickým formám environmentálnych stresorov. Oxidačný stres v koži je vo všeobecnosti spájaný hlavne s epidermálnymi a dermálnymi bunkami. Preto sa predpokladá, že tieto vrstvy sú najnáchylnejšie z hľadiska vzniku a poškodenia oxidačným stresom. Experimentálne sa dokázalo, že reaktívne formy kyslíka (ROS), ktoré vznikajú v dôsledku výkyvov prostredia, prispievajú k tvorbe ultra slabej fotónovej emisie (UPE) prostredníctvom oxidácie biomolekúl (nukleových kyselín, proteínov a lipidov). V posledných rokoch sa v rôznych štúdiách živých systémov (*in vitro*, *in vivo* a *ex vivo*) začali využívať techniky detekcie ultraslabých fotónov na štúdium oxidačného stresu. Výskum zameraný na dvojrozmerné fotónové zobrazovanie priťahuje čoraz väčšiu pozornosť vďaka svojej využiteľnosti ako neinvazívneho nástroja. Po exogénnej aplikácii peroxidu vodíka (H_2O_2) a/alebo Fentonovho činidla na kožné biopsie sme pozorovali výrazný rozdiel v stresom indukovanej a spontánnej emisii ultraslabých fotónov. Výsledky štúdie poukazujú na to, že konečnými emitentmi sú tripletový karbonyl ($^3C{=}O^*$) a singletový kyslík ($^1O_2$). Okrem toho, bola na ďalšie štúdium tvorby karbonylov a tvorby oxidačne modifikovaných proteínových aduktov po aplikácii H_2O_2 použitá imunoblotová analýza. Táto štúdia ďalej rozširuje naše chápanie mechanizmu, ktorý je základom tvorby ROS v koži vyvolanej oxidačným stresom, ako aj účasti/tvorby niekoľkých elektronicky excitovaných druhov, ktoré by potenciálne mohli byť využité ako nástroj pre určenie fyziologického stavu organizmu.

Kľúčové slová	prasačia koža, oxidačné radikálové reakcie, CCD zobrazovanie, dvojrozmerné zobrazovanie fotónovej emisie, malondialdehyd, oxidácia biomolekúl, proteínové modifikácie
Počet strán	41
Počet príloh	1
Jazyk	Anglický

Bibliographical identification

Author's first name and surname	Hana Duchová
Title	Formation of reactive oxygen species in skin cells
Type of thesis	Bachelor
Department	Department of Biophysics
Supervisor	doc. Ankush Prasad, Ph.D.
The year of presentation	2023

Abstract

The skin plays a pivotal role in many diverse bodily functions / processes, including metabolism, protection, thermoregulation, excretion, and sensation. All while being consistently exposed to both biotic and abiotic forms of environmental stressors. Oxidative stress in the skin is generally related to epidermal and dermal cells. Therefore, these regions are believed to be the most susceptible in terms of oxidative stress generation and damage. It has been experimentally proven that reactive oxygen species (ROS) formed due to environmental fluctuations contribute to the formation of ultra-weak photon emission (UPE) through the oxidation of biomolecules (nucleic acids, proteins, and lipids). More recently, different living system studies (*in vitro, in vivo*, and *ex vivo*) have utilized ultra-weak photon detection techniques to study oxidative stress. Two-dimensional photon imaging-centered research has been increasingly drawing attention due to its applicability as a non-invasive tool. Following the exogenous application of hydrogen peroxide (H_2O_2) and/or Fenton's reagent on skin biopsies we observed a marked difference in the stress-induced and spontaneous ultra-weak photon emission. The results of the study point to triplet carbonyl ($^3C=O^*$) and singlet oxygen ($^1O_2$) being the final emitters. Additionally, an immunoblotting assay was used to further study the carbonyl formation and the generation of oxidatively modified protein adducts after the application of H_2O_2. This study further broadens our understanding of the mechanism underlying the oxidative stress-induced generation of ROS in the skin, along with the contribution/formation of several electronically excited species that could potentially be used as a tool to determine the physiological state of the organism.

Keywords	pig skin, oxidative radical reactions, CCD imaging, 2-dimensional photon emission imaging, malondialdehyde, biomolecule oxidation, protein modification.
Number of pages	41
Number of appendices	1
Language	English

Contents

Aims

1. To better understand the formation of reactive oxygen species (ROS) formation in skin cells.
2. *Ex vivo* imaging of oxidative stress in skin biopsies and *ex vivo* model.
3. Immunoblotting – to understand the possible target of protein oxidation.
4. Data interpretation, data analysis, and its interpretation.

1   Introduction

Numerous important bodily processes/functions, such as sensory perception, thermoregulation, metabolism, excretion, hormones, and vitamin synthesis, can be attributed partially or entirely to the skin, the largest organ of the body (Wysocki, 1999). Furthermore, skin is the first mechanical barrier to the body's protection against invasive pathogens, dehydration, sun radiation, temperature fluctuations, and various chemical and mechanical attacks (Elias, 2007). Therefore, it is essential to study the mechanisms of the multitudinous roles the skin plays to discover novel effective treatments/procedures to maintain/restore its healthy condition.

To do this, researchers often turn to animal models as a form of representation of human skin. In addition to alleviating financial and ethical burdens, the variety of model systems and tools makes them an attractive alternative (Ericsson et al., 2013). These systems must have high levels of similarity to human skin in an attribute/part integral to a particular research objective. Pig skin ranks first (especially in dermatology) due to the countless anatomical, biochemical and physiological characteristics found in pigs and humans (Avon & Wood, 2005). Its advantage also lies in its wide accessibility and cost-effectiveness, as pork is the world's most produced/consumed meat (Clark & Tilman, 2017). Similarities are found from the multilayered skin composition, which can be grouped into three main layers: the epidermis, the dermis and the hypodermis (also called subcutis) (Debeer et al., 2013). The firm attachment of the integument, thickness and biochemical homologous identity of vital components such as porcine collagen (Summerfield et al., 2015). However, no animal model system shares all the characteristics of human skin in its entirety. For our study, porcine skin was chosen as an *ex-vivo* model with a comparable similarity to human skin in the essential characteristics to our research (such as its morphology and biochemical composition) than other available models. The skin is abundant in ROS like superoxide anion radical ($O_2^{\cdot-}$), H_2O_2, hydroxyl radical ($HO^{\cdot}$), and $^1O_2$ among others (Xu et al., 2017). This is due to both their endogenous and exogenous production/stimulation. The constant contact with molecular oxygen (O_2), xenobiotics, solar radiation, oxidative metabolism, immune cells destroying pathogens, psychological and physical stress are a few examples affecting the delicate natural oxidant/antioxidant balance in the cell and subsequently tissue/organ/organism (Rinnerthaler et al., 2015). If this condition is not restored through innate enzymatic and

non-enzymatic mechanisms/ exogenous antioxidants, it leads to a condition called oxidative stress (Sies, 2018). The eustress is attributed to ROS involved in cellular signaling, but the danger comes when the oxidative stress prevails, and important biomolecules like lipids, proteins and nucleic acids are negatively affected (Gasparovic et al., 2013). The biomolecule oxidation was found to be the cause/factor in formation/aggravation of several diseases like psoriasis, Alzheimer's disease, diabetes, and other mainly age-related diseases (Bizzozero, 2009; Sorolla et al., 2010). Oxidative stress-induced protein modifications are a common feature in several pathologies and are routinely used as a marker of oxidative stress along with malondialdehyde (MDA) which is a reactive carbonyl product of lipid peroxidation (Marrocco et al., 2017).

This study aims to learn more about oxidative stress-induced ROS generation in skin cells initiated through exogenous application of Fenton's reagent. Using a non-invasive sensitive tool, the charge-coupled device (CCD) camera, sodium ascorbate (singlet oxygen scavenger), and interference filter, we observed which excited species were formed and significantly contributed to the ultra-weak photon emission formation. The Fenton's reagent was selected due to its iron content (skin is rich in iron and other transition metals) and the ability to form a highly reactive HO· that initiates a cascade of reactions leading to eventual oxidative damage to lipids and proteins. Furthermore, immunoblotting using anti-MDA and anti-2,4-dinitrophenylhydrazone (DNP) antibodies was performed to observe protein carbonylation and proteins modified after lipid peroxidation following oxidative stress-induced ROS formation and lipid peroxidation.

2 The current state of the topic

2.1 Human and porcine skin: a comparison

As the largest organ in the body (approximately 2 m^2) and outermost mechanical barrier, the skin plays a vital role in numerous essential processes including thermoregulation, metabolism, excretion, and sensation (Wysocki, 1999). It provides protection from irradiation, biological and chemical aggressions, and fluctuating temperature among many other irritants (Rushmer et al., 1996; Bouten et al., 2005). In this regard, it is vital to fully understand the workings and effects of various types of stress to be able to devise new treatments and maintain the healthy condition of this organ.

For this purpose, multiple animal models have been used to obtain more information, as they possess remarkable anatomical, biochemical, and physiological similarities with human skin with lower financial, ethical, and availability constraints (Ericsson et al., 2013). Among these, the pig skin (also known as porcine skin) is considered an excellent model in many fields of biomedical research mainly due to its accessibility (the most prominent meat-producing livestock species worldwide), high genome and protein sequence homologies with humans, and a wide spectrum of available tools that can be applied (microarrays, ELISA, cell lines, antibodies) (Meurens et al., 2012; Clark & Tilman, 2017).

The similarities between human and porcine skin in terms of its anatomy, immune system, and physiology are profuse. In both species, skin is firmly attached to subcutaneous connective tissue and can be divided into three main layers: the avascular superficial layer (the epidermis), the collagen-rich elastic layer (the dermis), and the fatty innermost layer (the subcutis / hypoodermis) (Sullivan et al., 2001; Avon & Wood, 2005; Debeer et al., 2013). Most of the human epidermis is composed of densely packed cornifying squamous keratinocytes embedded in a hydrophobic lipid-enriched matrix that migrate through different epidermal layers from stratum basale to stratum corneum (the outermost layer) in the process of stratification. This process is essential for wound healing in humans and pigs, unlike most densely haired mammals, which heal primarily through wound contraction (Meyer et al., 1978; Sullivan et al., 2001; Strong et al., 2006; Proksch et al., 2008;). The rest of the epidermis consists of Merkel mechanoreceptor cells (rarer in pigs), pigment-producing cells (melanocytes in man) and antigen-presenting Langerhans cells (Debeer et al., 2013). The thickness of this layer is another example of shared similarity with 60-120 µm in man and 30-100/70-140 µm depending on the body site in pig (Meyer et al., 1978; Rushmer et al., 1996; Hammond et al., 2000; Sandby-

Møller et al., 2003). The underlying connective tissue, the dermis, is connected by the basement membrane and is subdivided into two zones: the papillary dermis (usually in contact with the rete ridges of the epidermis through the basement membrane) and the reticular layer (in contact with the hypodermis). The main components are fibroblast, cells secreting all extracellular proteins, including collagen and elastin, that provide the characteristic elasticity of the skin (Meyer et al., 1978; Rushmer et al., 1996; Debeer et al., 2013). The rest include dendritic and mast cells. In addition to these, the human dermis is richly innervated and abundantly stocked with lymphatic and blood vessels. In pigs, the dermal vascular structure is slightly richer; however, the collagen fiber content was reported to be sparser with slightly thinner fibers. Despite this, the biochemical identity of porcine collagen is homologous to that of humans (Heinrich et al., 1971; Rushmer et al., 1996; Debeer et al., 2013; Starcher et al., 2005; Wang & Sanders, 2005). Differences can be seen in the absence of eccrine glands and in the more outward distribution of apocrine glands in porcine skin compared to human skin. Dermal hair follicles have been reported to have similarities between the two species (Debeer et al., 2013). The interface between the skin and the underlying structures, the subcutaneous fat, is mostly composed of lipids and fatty acid-filled adipocytes. This layer is well vascularised, although typically thicker in pigs (Avon & Wood, 2005; Wang & Sanders, 2005; Debeer et al., 2013).

Based on the remarkable likeness, specifically with respect to the epidermis and dermis, the porcine skin was selected as the best suited *ex vivo* model for human skin in this study.
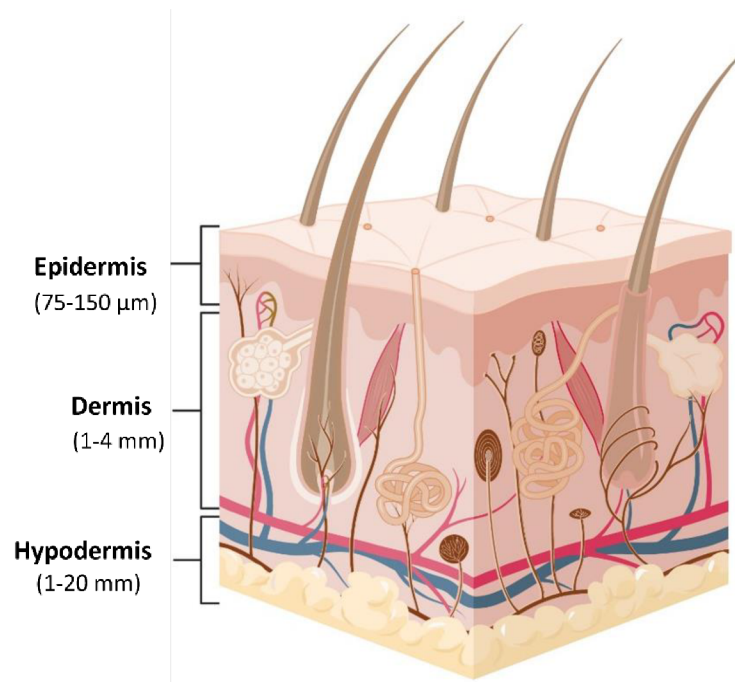
Figure 1 : A schematic representation of skin anatomy. The layers show the epidermis (the top layer) the dermis (the middle layer), and the hypodermis (the lower fatty layer). The stratum corneum is the topmost layer of the epidermis and ranges from 10 to 30 µm. Presented figure was created using Biorender.com.

2.2 Reactive oxygen species and oxidative stress in skin

Reactive oxygen species are omnipresent in living organisms, and skin oftentimes being amongst the most saturated organs. The formation of these derivatives can be done through two types of mechanisms. The first is the electron transport from highly reducing compounds to molecular oxygen, as is the case of $O_2^{\bullet-}$, which in turn can be reduced to H_2O_2 and highly reactive $HO^{\bullet}$. The second pathway involves excitation energy transfer to O_2 which is linked to triplet chromophores and generates singlet oxygen (Turrens, 2003; Barry Halliwell & Gutteridge, 2015).

In the skin, ROS occur not only as products and by-products of endogenous enzymatic processes but can also be formed due to various biotic and abiotic environmental stressors (Rinnerthaler et al., 2015) (Fig. 1). Enzymatic sources are namely the NADPH oxidases, peroxisomal oxidases, cyclo- and lipoxygenases xanthine oxidoreductase (XOR), and enzymes of the cytochrome P450 family. Environmental influences include numerous pollutants, metal ions (especially iron), irradiation by ultraviolet (UV) light, and xenobiotics (Chen et al., 2012; Poljšak & Dahmane, 2012; Rinnerthaler et al., 2015).

In mitochondria, up to 1-2% of the overall O_2 intake is converted into superoxide ($O_2^{\bullet}$) (Turrens, 2003). However, the epidermal mitochondrial contribution to ROS production has a decreasing tendency as organelles in keratinocytes degenerate during cornification (Holbrook, 1989; Jeon et al., 1998). The endoplasmic reticulum (ER) and peroxisomes contain/are associated with an extensive range of enzymes amongst which flavoenzymes/oxidoreductases are the most significant in ROS production due to the presumed formation of H_2O_2 and/or $O_2^{\bullet-}$ as a byproduct (Huber et al., 1987; Fransen et al., 2012). The ER is also associated with oxygen radical generation due to the cytochrome P450 family and NADPH detoxification activity (Gorsky et al., 1984; Baron et al., 2001; Yengi et al., 2003; Bae et al., 2011). The production of ROS in the ER and peroxisomes is understood to be the same/higher as that of mitochondria, making them the main contributors to ROS generation in the cell along with mitochondria (Fransen et al., 2012). Membranes such as the plasma membrane as well as mitochondrial, and ER owning to the present NADPH oxidases, can also produce ROS (Baron et al., 2001; Block et al., 2009; Rinnerthaler et al., 2012; Pospíšil et al., 2019). The metabolism of arachidonic acid and the oxygen-iron ions reactions are the main sources of ROS in the cytosol (Winston et al., 1984; Korbecki et al., 2013; Rifkind et al., 2015). Reactive oxygen species like $HO^{\bullet}$ are generated through Fenton reaction when ferrous ion reacts with H_2O_2 (Gupta et al., 2016).

The exogenous ROS formation-inducing factors are multiple, which can be attributed mainly to the position of this organ. Acting as the outermost layer, the skin, is constantly interacting with the environment, where contact with pollutants, xenobiotics, and solar radiation is inevitable. However, unhealthy diet, severe psychological and physical stress, and cigarette smoke were similarly found to belong to this category (Martin & Barrett, 2002; Poljšak & Dahmane, 2012; Pisoschi et al., 2021).

To compensate for the numerous previously mentioned endogenous and exogenous ROS sources, the skin is armed with both enzymatic and non-enzymatic anti-oxidative mechanisms. The epidermis was observed to be more saturated with antioxidants than the underlying dermis. Low-molecular weight antioxidants like vitamin C, vitamin E, glutathione, ubiquinol, and uric acid are the most prominent (Weber et al., 1999; Dobrakowski et al., 2016; Pisoschi et al., 2021). The proteins of the Small repeat rich in prolines (SPPR) family (especially the SPPR2 subfamily) found in the cornified envelope were found to quench ROS by the formation of intramolecular disulfide bonds (Rinnerthaler et al., 2013). Enzymatic defense is represented in the form of superoxide

dismutases (SODs), catalases, ferritin, glutathione peroxidases, and peroxiredoxins (Chiumiento & Bruschi, 2009; J. Zhang et al., 2020).

2.3 Oxidative stress and biological targets of ROS

By disrupting the organism's intrinsic balance between the formation of ROS and its ability to safely counteract them/their reactive intermediates, the state called oxidative stress is induced. The intensity of this stress reflects either eustress, which is formed by a naturally occurring increase in ROS as messengers during redox signaling, or toxic oxidative stress resulting in damage to three main targets: proteins, lipids, and nucleic acids (Sies, 2018). The oxidation of these biomolecules can typically be traced to either radical-induced or nonradical-induced oxidation. Radical-induced oxidation is characterized by the formation of radicals initiated by hydrogen transfer (usually its abstraction from the biomolecule) due to the presence of a radical species. The name, non-radical oxidation, reflects the involvement of non-radical species in this type of oxidation. It is mainly related to singlet oxygen and subsequent oxygenation of a biomolecule (oxygen addition), resulting in the production of an oxygenated biomolecule (Gasparovic et al., 2013; Pospíšil et al., 2019). The minimal reactivity and oxidizing capability of H_2O_2 prevent it from having a significant role in non-radical oxidation. However, its stability and low reactivity provide H_2O_2 with a long lifespan, which in combination with its ability to generate a highly oxidizing species like $HO^{\bullet}$ is what makes H_2O_2 potentially damaging (Halliwell et al., 2000; Dahlgren et al., 2007).

Lipid peroxidation can be initiated by an attack on the fatty acid/fatty acyl side chain - polyunsaturated fatty acids (PUFAs), which are particularly susceptible to hydrogen abstraction. Trace metals (especially iron) along with ROS generate a pool of reactive peroxyl radicals ($ROO^{\bullet}$) which in turn react with neighboring lipids (Sadrzadeh et al., 1984; Halliwell et al., 1993). This continuous H-abstraction and oxygenation most often leads to a chain reaction that can propagate until it is terminated by radical recombination or antioxidant activity. This process is known to generate stable cytotoxic aliphatic aldehydes, namely 4-hydroxy-2-nonenal (HNE) and malondialdehyde, as well as other aldehydes, acrolein, and heptanal (Poli et al., 1985; Halliwell et al., 1993; Schneider et al., 2008; Guéraud et al., 2010). Lipid peroxidation damage to phospholipid membranes negatively affects their permeability and allows the reactive products to spread further into the cell/out of the cell, and therefore affect other crucial structures by forming adducts (Halliwell et al., 1993).

Alterations in DNA resulting from oxidants include sister chromatid exchange, base and abasic site modifications, strand breaks, and formation of DNA-protein crosslinks. Subsequently, mutations, errors in replication, genomic instability, and eventually cell death can occur (Klaunig et al., 2010; Poljšak & Dahmane, 2012).

2.3.1 Protein modification

The skin is also abundant in different proteins that assist in fulfilling the numerous essential functions of this organ. Recently, a robust proteome study by Dyring-Andersen et al., (2020) identified a total of 10,701 proteins in the three layers that form human skin. Their ampleness is one of the most notable features that makes proteins ideal targets of oxidative damage. It is understood that proteins can be oxidised directly at their backbone/amino acid side chains or indirectly through secondary products of lipid oxidation (especially HNE and MDA) or carbohydrate oxidation. This can result in numerous alterations with respect to their structure and function (Fedorova, 2017).

The term most associated with oxidative stress-induced protein modifications is 'protein carbonylation'. The defining feature of this process is carbonyl group (C=O) formation, which arises from the types of oxidative stress reactions. Among the first causes of carbonylated protein formation, historically, was Fenton reaction-generated $HO^{\bullet}$ mediated oxidation (metal-catalyzed oxidation) of arginine, proline, threonine, and lysine amino acid side chains (Oliver et al., 1987; Fedorova, 2017). Generally, histidine, leucine, cysteine, methionine, tyrosine, tryptophan, and phenylalanine are examples of amino acids that are more prone to oxidation than other residues. Considering that these alterations occur early on in oxidative stress-induced reactions and most of them are irreversible and therefore very stable, their presence is a widely recognised marker of oxidative stress.

The lack of distinct fluorescence of these markers hinders direct detection. However, several detection techniques have been proposed over the years. Among them are spectrometry, immunocyto-/histochemistry, enzyme-linked immunosorbent assay (ELISA), and western blot approaches following C=O derivatization with hydrazines / hydrozides / hydroxylamines (Yan & Forster, 2011). The introduction of soft ionisation techniques such as matrix-assisted laser desorption/ionisation (MALDI) or electrospray ionisation (ESI) combined with tandem mass spectrometry (MS/MS) allowed for specific protein carbonylation types and side modification detection (Bollineni et al., 2011).

The oxidative damage at the protein level can be further divided by the severity of the damage. Slight oxidation can decrease protein activity and thermostability; however, members of cellular oxidative stress protection mechanisms (eg, thioredoxin) are usually able to repair this level of damage (Arnér & Holmgren, 2000; Naskalski & Bartosz, 2001). If these mechanisms prove to be insufficient, the modifications multiply and the proteins begin to unfold and lose their activity. Substantial unfolding allows for cross-link formation leading to small aggregates, which can be either be degraded by the proteasome or refolded through the activity of the heat shock protein family (Höhn et al., 2013). With continued oxidation and accumulating aggregation, a point where proteasome is unable to degrade or its activity is completely inhibited (owing to mechanical or the steric inhibition or size of the clusters). Aggregates can also incorporate lipids and at later age even carbohydrates. This is known as lipofuscin, alternatively 'ceroid' or "age pigment" which cumulates in all cell types, including those of the skin (predominantly in the dermis). The protein-lipid clusters comprise 30-70% proteins and 20-50% lipids and can bind metals/metal-containing proteins which promote HO$^\bullet$ formation that in turn contributes to further oxidation. Therefore, the vicious oxidation cycle continues and can eventually lead to apoptosis of the parent cell/nearby cells/tissues and even organs (Rinnerthaler et al., 2015).

2.3.2   A consequence of skin oxidation in relation to disease

Although low to medium concentrations of ROS were shown to be essential regulators/stimulants of biological processes such as wound healing, pathogen defence, neoangiogenesis (low levels of H_2O_2), cell growth and proliferation, intracellular signaling, and the activity of several transcription factors, it is crucial to retain the delicate redox balance in the cell. (Roy et al., 2006; Wu, 2006; Sen & Roy, 2008). Higher concentrations and/or prolonged pro-oxidative states in the cell can spread into adjacent cells and can lead to oxidative stress-induced aggravation of physiological and pathological processes. These include ageing, inflammation, autophagy, and apoptosis, leading to the development of numerous diseases and even malignancies. It is well established that oxidative stress-induced lipid peroxidation is involved in atherosclerosis and rheumatoid arthritis (Esterbauer & Hpuhl, 1993; Gambhir et al., 1997). Protein carbonylation was also found to be linked to a variety of age-related and neurodegenerative diseases, including Huntington's disease, Parkinson's disease, Alzheimer's disease, diabetes, dementia, and multiple/amyotrophic lateral sclerosis

(Bizzozero, 2009; Sorolla et al., 2010; Hecker & Wagner, 2018). Other examples of protein carbonyl-associated pathologies are sepsis, respiratory distress syndrome, metabolic syndrome, obesity, cystic fibrosis, and chronic renal failure (Dalle-Donne et al., 2003; Fedorova, 2017).

Similarly, oxidative stress and the damage associated with it can be found at the root of various skin diseases. Specifically, inflammatory skin diseases and diseases such as psoriasis and vitiligo (Xu et al., 2018). Skin is more susceptible to ageing and the ageing process is driven by ROS at a significantly higher level than in any other organ that has constant contact with atmospheric oxygen and relatively high endogenous ROS production (Rinnerthaler et al., 2015). Melanocytes were found to produce more of them than other skin cells. This is surprising given the ROS-scavenging activity of melanin. Even more interesting was the finding that it is melanogenesis and low melanocyte oxidative repair ability of melanocytes that cause melanocytes to be persistently under oxidative stress – melanogenesis stress. The low repair capability, especially in terms of DNA damage, makes them susceptible to melanoma formation and activates proto-oncogenic pathways (Fruehauf & Trapp, 2008). DNA repair defects after oxidative damage to the skin were also found to be involved in the development of Xeroderma pigmentosum disease, which is known to cause a significant increase in both photosensitivity and the incidence of sun-induced skin cancer (Niedernhofer et al., 2011).

However, photodynamic therapy (PDT) represents a positive aspect of ROS generation. In this type of clinical therapy, first, a photosensitiser in the form of cream/injection/imbibed liquid is administered. Its role is to accumulate in affected cells/tissue and upon activation by a specific light source, transfer energy to nearby oxygen-containing substrates such as water / O_2. This transfer promotes increased ROS production that specifically targets and eventually kills cancerous cells without damaging surrounding healthy cells. The workings behind PDT is that cancer cells generally overproduce the ROS and, therefore, antioxidants are upregulated to maintain the redox state below the toxic level. However, by adding exogenously produced ROS (through the administered photosensitizers and light activation), the scales are tipped in favor of the oxidants and the cells die. The difference in the redox state of diseased and normal cells allows for targeted treatment of several types of skin cancer as well as other types of cancer. Examples are basal cell carcinoma, squamous cell carcinoma, and glioblastoma (Zhou et al., 2016; Karges, 2022).

2.4   Methods for oxidative stress detection in skin

Among environmental stresses to the skin, oxidative radical reactions have been the focus of an increasing number of studies, especially in the past few decades (Sander et al., 2002; Rifkind et al., 2015b; Rinnerthaler et al., 2015; Ji & Li, 2016). Through exploration, numerous markers of oxidative stress have been discovered, which significantly facilitated linking this type of stress with the development and/or progression of various pathologies. Oxidative stress has also been measured directly through ROS detection and characterization.

Direct ROS detection is challenging because of their generally high reactivity and a very short lifespan. For this reason, highly sensitive detectors and fast response techniques must be employed. These include electron paramagnetic resonance (EPR) spin-trapping spectroscopy, where the complication of a short ROS lifetime is overcome by the addition of a spin trap that allows its detection by extending the lifetime of the radical. Other examples are chemiluminescent/fluorescent probes - require oxidation for luminescence/fluorescent emission e.g., luminol and dihydroethidium (DHE) staining, chromatography methods – with the usage of reagent (e.g., salicylic acid) which is used for ROS stabilization and the technique is usually combined with spectroscopy methods – capable of semi-quantification of free radicals, fluorescent proteins – recombinant proteins that after introduction to the cell localizes at defined sites and reflect the redox state of a specific region through fluorescence, after its oxidation and consequential structural reformation (e.g., HyPer), and fluorescent biosensors – sensitive and selective method for monitoring real-time radical formation (Zhang et al., 2018).

Biological systems naturally emit light, owning to photon emission formed when electronically excited molecules return to their ground states in metabolic processes; this is called ultra-weak photon emission or biophoton emission. Considering that ultra-weak photon emission intensity is known to be affected due to ROS formation (especially $^1O_2$ and $^3C=O^*$ associated with oxidative stress reactions (oxidation of biomolecules), observation of the changes in this emission could reflect the oxidative state of the skin. One of the methods used for measuring the UPE intensity is a highly sensitive CCD camera, that allows spatiotemporal two-dimensional imaging. By employing specific interference filters, it is possible to identify the spectral distribution of this emission and, therefore, the excited species involved in its formation. The excited species emit light throughout the spectrum, $^3C=O^*$ in the areas near UVA and blue-green areas (350-550 nm), $^1O_2$ in the red (634 and 703 nm) and near IR (1270 nm) areas, and the singlet excited

skin pigments (melanin and bilirubin) emit in the broad range from 550–600 nm covering the green region of the spectrum (Prasad & Pospišil, 2011; Rastogi & Pospíšil, 2011; Prasad & Pospíšil, 2013; Cifra & Pospíšil, 2014; Pospíšil et al., 2019; Prasad et al., 2018).

Unlike previously mentioned direct ROS detection methods, and UPE measurement, which represents a potential tool for non-invasive oxidative state monitoring, the most widespread methods for oxidative stress detection, especially in clinical research are methods detecting more stable products originating from ROS-induced oxidation of biomolecules (Kehm et al., 2021). These products must not only be stable, but also accumulate in detectable concentrations reflecting the gravity of the disease to be considered biomarkers. Modifications of oxidized proteins, such as carbonylation, glycoxidation, or lipoxidation, typically have associated biomarkers. As mentioned previously, biomarkers such as protein carbonyls, HNE and MDA are routinely used for oxidative stress detection/identification/quantification in blood, urine, or cell/tissue samples like skin lysate, and the means through which the data are obtained range from spectrometry, immunohistochemistry, Western blot, and ELISA to HPLC, MALDI, and MS methods (Ohkawa et al., 1979; Bollineni et al., 2011; Hawkins & Davies, 2019; Kehm et al., 2021; Masutin et al., 2022).

In contrast to MDA detecting/quantifying techniques where the lipid peroxidation product is measured directly, the methods used to assess protein carbonylation content usually call for sample derivatization prior to measurements (Yan & Forster, 2011). For this purpose, probes like DNPH (sometimes also called Brady's reagent) are generally mixed with the sample to form stable dinitrophenyl groups (DNP) (Levine et al., 1990; Tsiropoulou & Touyz, 2017). The DNP groups are formed when the DNPH molecules react with carbonyl groups in the sample, and the formed yellow product can be spectrophotometrically detected. The characteristic absorption maximum of these DNP adducts occurs at 365–375 nm (Levine et al., 1990). Besides spectrophotometric methods, other previously stated techniques like HPLC, MS methods as well as Western blot and ELISA were successfully used after the protein derivatization and the development of DNP-specific antibodies (Buss et al., 1997; Morgan et al., 2007).

3 Materials and Methods

3.1 Chemicals

The chemicals used in the study along with their given suppliers are listed in table 1.

Table 1: Complete list of chemicals used with the name of the supply company.

Product	Supplier
2-mercaptoethanol	Sigma-Aldrich Chemie GmbH, Germany
Bovine serum albumin (BSA)	Sigma-Aldrich Chemie, GmbH, Germany
Bromophenol blue	BDH Laboratory Supplies, UK
Chemiluminescent horseradish peroxidase (HRP) Substrate	Sigma-Aldrich Chemie, GmbH, Germany
Dithiothreitol (DTT)	Thermo Fisher Scientific, Paisley, UK
Glycerol	Lach-Ner, Czech Republic
Hydrogen peroxide	Sigma-Aldrich Chemie GmbH, Germany
Iron (II) sulfate heptahydrate ($FeSO_4 \cdot 7H_2O$)	BDH Laboratory Supplies, UK
Ponceau stain	Abcam, Cambridge, UK
Protease inhibitors tablets	Roche, Switzerland
Sodium ascorbate	Sigma-Aldrich Chemie GmbH, Germany
Sodium chloride (NaCl)	Penta chemicals, Czech Republic
Sodium deoxycholate	Sigma-Aldrich Chemie GmbH, Germany
Sodium dodecyl sulphate (SDS)	BDH Laboratory Supplies, UK
Tris(hydroxymethyl)aminomethane (TRIS)	Sigma-Aldrich Chemie GmbH, Germany
Triton X-100	Sigma-Aldrich Chemie GmbH, Germany
Tween 20	Sigma-Aldrich Chemie GmbH, Germany

3.2 Buffers and solutions

3.2.1 Fenton's reagent and Singlet oxygen scavenger

A solution of ferrous sulphate and hydrogen peroxide was used to prepare Fenton's reagent. A set concentration and volume of $FeSO_4$ (100 µl, 250 µM) and varying concentrations of H_2O_2 (10 mM, 5 mM, or 2.5 mM) in a fixed volume of 250 µl were applied to a blotting paper placed on the surface of skin samples (intact porcine ear/skin biopsies) in all the CCD camera masurements. Blotting paper allowed complete control over the size and location of the treatment site. Singlet oxygen scavenger Sodium ascorbate was used in the form of a 10 mM solution. Samples were treated with Sodium ascorbate 10 min prior to the application of Fenton's reagent.

3.2.2 Radioimmunoprecipitation assay (RIPA) buffer

- 1x (v/v) complete protease inhibitor cocktail
- 150 mM NaCl
- 1% NP-40
- 1x (v/v) phosphatase inhibitor
- 0.1% SDS
- 0.5% sodium deoxycholate
- 50 mM tris, pH 8,0

3.2.3 Neutralization buffer for DNPH derivatization

- 30% (v/v) glycerol
- 2 M tris

3.2.4 Reducing sample buffer (5x)

- 0.02% bromophenol blue
- 6% (v/v) DTT
- 30% (v/v) glycerol
- 12% (w/v) SDS
- 150 mM tris

3.2.5 Phosphate-buffered saline (PBS) buffer (10x) (pH 7.4)

- 100 mM dibasic dodecahydratesodium phosphate ($Na_2HPO_4·12H_2O$)
- 28 mM KCl
- 18 mM Monopotassium phosphate (KH_2PO_4)

- 1.4 M NaCl

3.2.6 Phosphate-buffered saline with Tween 20 (PBST)
- 1x PBS with 0,1% of Tween 20

3.2.7 Blocking buffer
- 5% BSA in PBST buffer

3.3 Molecular weight marker
- PageRuler™ Plus pre-stained protein ladder (10-250 kDa) (Thermo Fisher Scientific, Massachusetts, USA)

3.4 Antibodies
- Rabbit polyclonal anti-MDA primary antibody (Abcam, UK)
- Rabbit polyclonal Dinitrophenyl-KLH antibody (anti-DNP) (ThermoFisher scientific, MA, USA)
- Goat anti-rabbit HRP conjugated secondary antibody (Bio-Rad Laboratories, California, USA)

3.5 Diagnostic kits
- Pierce BCA protein assay kit (Thermo Fisher Scientific, Paisley, UK)

3.6 Appliances
- Amersham Imager 600 (GE Healthcare, UK)
- Analytical balance KERN ABT 220-5DM (KERN & SOHN GmbH)
- Automatic pipettes (Eppendorf, Germany)
- BioTek Synergy Mx Microplate Reader SMA (Agilent, California, USA).
- CCD camera VersArray 1300B (Princeton Instruments, NJ, USA)
- Centrifuge 5430 R (Eppendorf, Germany)
- IKA T25 basic homogenizer (IKA, Germany)
- Interference filter type 644 (Schott & Gen., Germany)
- Trans-Blot Turbo Blotting System (Bio-Rad Laboratories, California, USA)

3.7 Software
- ImageJ (National Institutes of Health, Maryland, USA)
- PowerPoint 365 (Microsoft Corporation, Washington, USA)

- Excel 365 (Microsoft Corporation, Washington, USA)

- Andor Solis (Andor Technology Ltd, Belfast, UK) Biological material

- BIORENDER (Toronto, Canada; https://biorender.com/)

3.8 Biological material

3.8.1 Porcine skin samples

Intact pig ears were provided by a local slaughterhouse (Olomouc, Czech Republic). Fresh samples were delivered to the laboratory in an icebox to maintain a low temperature and were used the same day. In all experiments either an entire pig ear or a skin biopsy, prepared following the procedure described in Chiu & Burd, (2005) with minor moderations, was used. Illustrative photographs of a whole pig ear (A) with indicated area from which skin biopsy can be isolated from a cut-out (B) are shown in Figure 2 below.
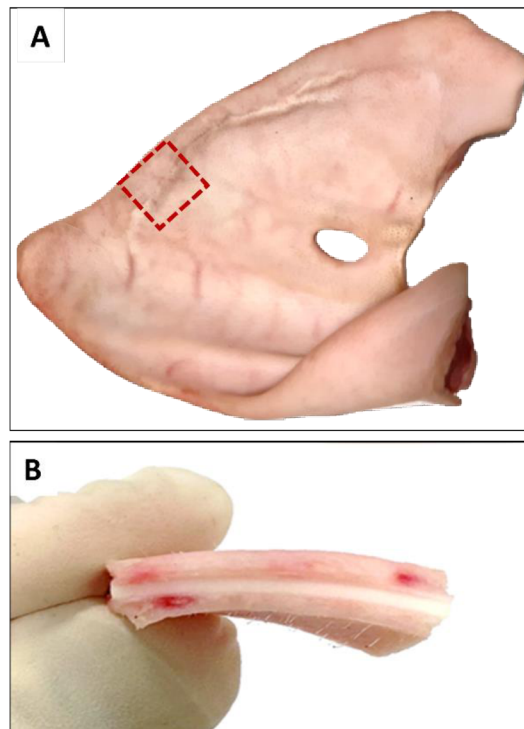

Figure 2: Photographs of intact porcine ear (A) and porcine skin cut-out portion showing the layers (B).

3.9 The experimental setup

A specially designed dark room is required for the measurement of ultra-weak photon emission to circumvent the interference of stray photons. In this regard, the ultra-weak photon emission measurements in our study were done in an experimental darkroom following the conditions described previously by Prasad & Pospíšil, (2013) (Fig. 3).

3.9.1 Fenton's reagent and the measurement of the UPE

Preceding the start of the measurements (~3 min), Fenton´s reagent, prepared as previously described (250 µM solution of $FeSO_4$ and 10 mM, 5 mM, or 2.5 mM H_2O_2), was topically applied to skin biopsies/intact ear. The aforementioned concentrations of Fenton´s reagent and combination of the reagent following a pre-treatment with 10 mM Sodium ascorbate (10 min preceding application of Fenton's reagent) were used to observe the change in ultra-weak photon emission.
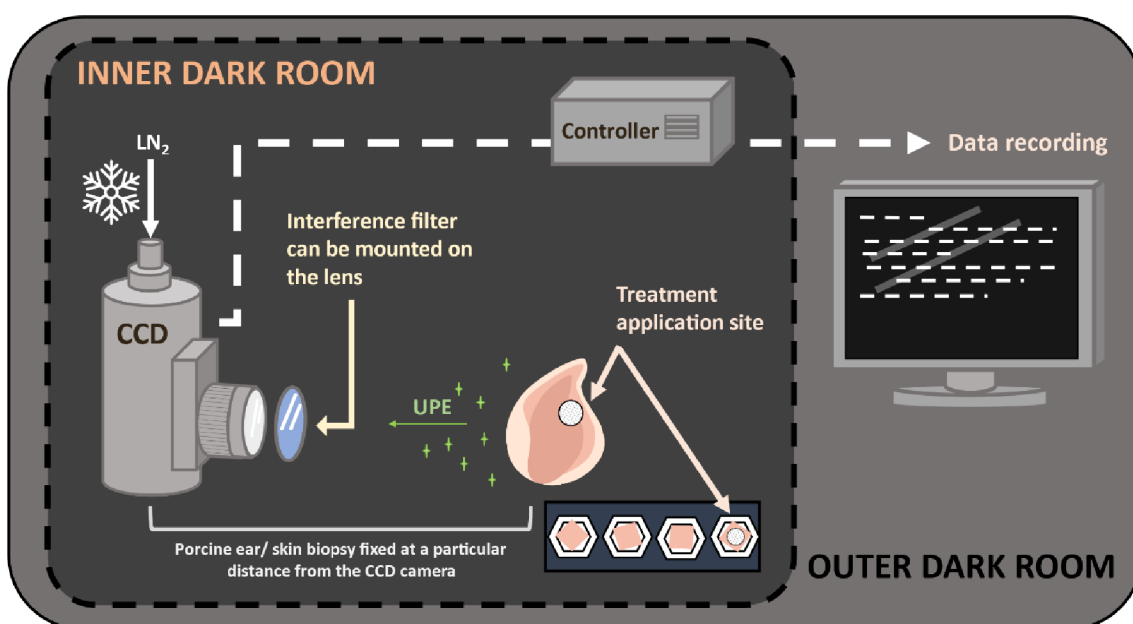

Figure 3: Schematic diagram of the working arrangement for two-dimensional photon emission imaging using a CCD camera. Inner dark room (dark gray) and the outer control room (green) are indicated. The interference filter was positioned in front of the objective lens for the spectral measurements as shown. Figure adopted with modifications from Prasad et al., 2023.

3.9.2 CCD camera measurements

Two-dimensional imaging of ultra-weak photon emission was done using a highly sensitive CCD camera for all samples (porcine ear/skin biopsies). Before measurements were made, the samples were kept in the dark for a minimum of 10 min to prevent any kind of interference caused by delayed luminescence. In our study, CCD camera VersArray 1300B of the spectral sensitivity 350-1000 nm and nearly 90% quantum efficiency in the visible range of the spectrum was used and the following conditions were employed: gain, 2; scan rate, 100 kHz; an accumulation time, 30 min. Liquid nitrogen was used to cool down the CCD camera to a working temperature of -105 °C, as well as reduce the thermionic emission on the photocathode and subsequently minimize the dark current. Data correction was made for each measurement by subtracting background noise (dark count).

3.9.3 Contribution of ^{3}C=O* in Fenton's reagent induced UPE formation

An interference (dichroic) filter type 644 with transmission range 340-540 nm was mounted on the CCD camera lens to monitor the contribution of ^{3}C=O* in Fenton's reagent induced ultra-weak photon emission. The choice of the filter was based on the ^{3}C=O* emission (350-550 nm) in the blue-green region of the spectrum. Measurements with the filter were carried out in the same manner as was previously described.

3.10 Protein whole skin tissue lysate preparation

Skin is a very tough tissue and therefore a thorough homogenization protocol is needed for the preparation of protein lysate. Skin biopsies (0.5 g) were prepared, cut to smaller pieces, and divided into 3 sets based on the following treatment: Control samples (no treatment), 10 mM H_2O_2 treated samples, and Fenton's reagent treated samples (250 µl of 10 mM H_2O_2 + 100 µl of 250 µM $FeSO_4$). Biopsies were treated in the dark for 30 min (on ice). After removing the chemicals, skin biopsies were shortly submerged in liquid nitrogen, and RIPA) buffer (3 ml) was added. Samples were subjected to homogenization (3 cycles, each for 1 min) followed by 3 cycles of centrifugation at 4°C for the obtained supernatants [30 min at 7 745 g (7 830 rpm) and 2x 45 min at 17 970 g (14 000 rpm)]. Final supernatants were collected and used for further experiments.

3.10.1 Protein Assay

The protein concentration of collected supernatants was estimated using the Pierce bicinchoninic acid (BCA) protein assay kit. Seven BSA standards (125, 250, 500, 750,

1500, 2000 mg·ml^{-1}), RIPA buffer (as a blank), and the supernatants were loaded onto a 96-well microplate (working volume was 10 µl). Following the user guide, 200 µl of the working BCA reagent were added. The microplate was covered in aluminum foil and incubated at 37°C for 30 min. Afterwards, it was let to cool down to room temperature (RT) and absorbance was measured (at 562 nm) on a plate reader. Flowchart of the workflow from tissue lysate preparation to protein estimation is shown in Fig. 4.

3.10.2 Calculation of protein concentration from the standard curve

Standard curve was generated by plotting the average absorbance values (562 nm) of all individual BSA standards (y-axis) and their corresponding concentrations in µg/ml (x-axis). Trend line equation in a format: y = ax + b was used to determine the protein concentration of whole-tissue skin lysates by solving for x. Obtained absorbance values of protein samples were corrected by subtracting the blank average before calculations. The BSA standard curve (Fig. 5) along with the final protein concentrations and other relevant information delineating the skin extracts presented in Table 2 are for representation only, and calculations were repeated for each protein isolation.
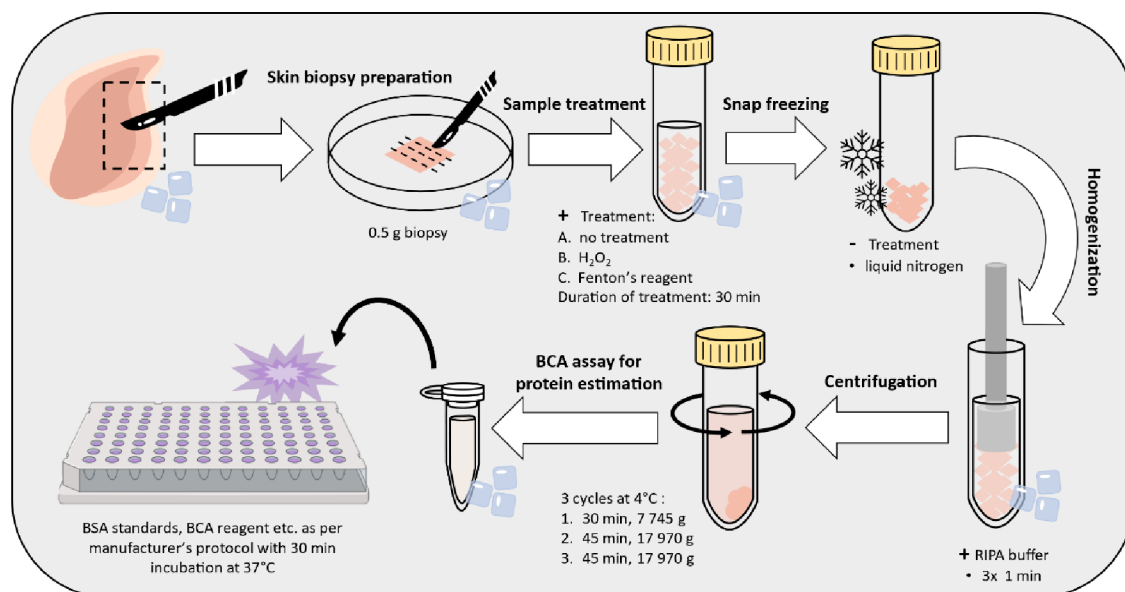

Figure 4: Flowchart depicting the workflow of whole-skin tissue lysate preparation and BCA Assay protein estimation. BSA – Bovine serum albumin, H_2O_2 – Hydrogen peroxide RIPA - Radioimmunoprecipitation assay buffer. Adopted with modifications from Prasad et al., 2023.
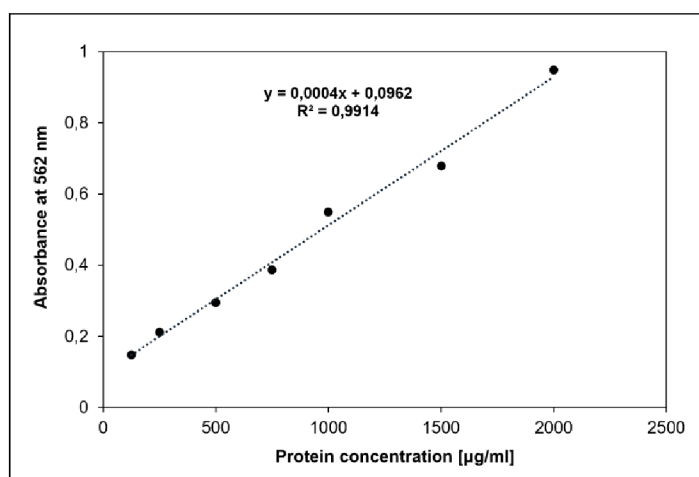
Figure 5: BSA Standard curve calculated from obtained absorbance values at 562 nm (y-axis) and corresponding protein concentrations of BSA standards in μg/ml (x-axis).

Table 2: Representative values for Pierce™ BCA Protein Assay Kit quantification of total protein concentration from standard curve (Fig. 5) in porcine skin extracts

Samples	Treatment	Absorbance (OD_{562})	OD_{562} - Blank	Protein concentration [μg/ml]
Control 1	-	0.602	0.5305	1085.75
Control 2	-	0.581	0.5095	1033.25
Control 3	-	0.481	0.4095	783.25
Hydrogen peroxide 1	10 mM H_2O_2	0.452	0.3805	710.75
Hydrogen peroxide 2	10 mM H_2O_2	0.552	0.4805	960.75
Hydrogen peroxide 3	10 mM H_2O_2	0.54	0.4685	930.75
Fenton´s reagent 1	500 μM $FeSO_4$ + 10 mM H_2O_2	0.547	0.4755	948.25
Fenton´s reagent 2	500 μM $FeSO_4$ + 10 mM H_2O_2	0.526	0.4545	895.75
Fenton´s reagent 3	500 μM $FeSO_4$ + 10 mM H_2O_2	0.566	0.4945	995.75
Blank OD_{562} average			0.0715	

3.11 Sample preparation for Western blot analysis of MDA

The whole skin tissue homogenate extracted from sets of porcine skin biopsies treated with untreated, 10 mM H_2O_2 and Fenton's reagent (10 mM H_2O_2 and 500 µM $FeSO_4$) treated porcine skin biopsies was combined with 5x loading buffer and boiled at 70°C for 10 min. The molecular weight marker and a uniform amount (10 µg) was loaded onto 10% SDS-PAGE gel and separated. Bands were electroblotted onto a nitrocellulose membrane using Trans-Blot Turbo Blotting System.

3.12 Sample preparation for Western blot analysis of carbonylated proteins using DNPH

Unlike MDA, the 3 types of samples required derivatization before their electrophoretic separation. Therefore 20 µl of each sample was combined with equal volume of 15% SDS, and 40 µl of 50 mM DNPH. After a short vortex, the solution was left 30 min in the dark for incubation. The derivatization was neutralized by adding 20 µl of neutralisation buffer following the incubation period. The molecular weight marker and a uniform amount (30µl = 6 µg of protein) was loaded onto 10% SDS-PAGE gel and separated. The bands were electroblotted to a nitrocellulose membrane using a Trans-Blot Turbo Blotting System.

3.13 Ponceau staining and Western blot analysis of MDA and DNP

The membranes were incubated with the Ponceau stain solution for ~5 min, gently washed with distilled water, and stained protein bands were captured with Amersham Imager 600. After washing out the stain, the membranes were left to incubate overnight at 4°C in 5% BSA in PBST. The blocked membrane was then incubated with rabbit anti-MDA primary antibody/ anti-DNP (1:5000 in blocking buffer) (2 h, on a rocker at RT. Four 5-min washing cycles (PBST) were followed by incubation with the goat HRP-conjugated anti-rabbit secondary antibody (1:10 000 in blocking buffer) (1 h, rocker at RT). 5-min washing cycles (5x) in PBST were performed before adding the Immobilon Western Chemiluminescent HRP substrate. Chemiluminescent signal imaging was done using Amersham Imager 600. Figure 6 below summarizes the workflow of western blotting from the initial sample preparation for SDS-PAGE to the final signal imaging. The quantification of protein band density (densitogram) was done using ImageJ software.
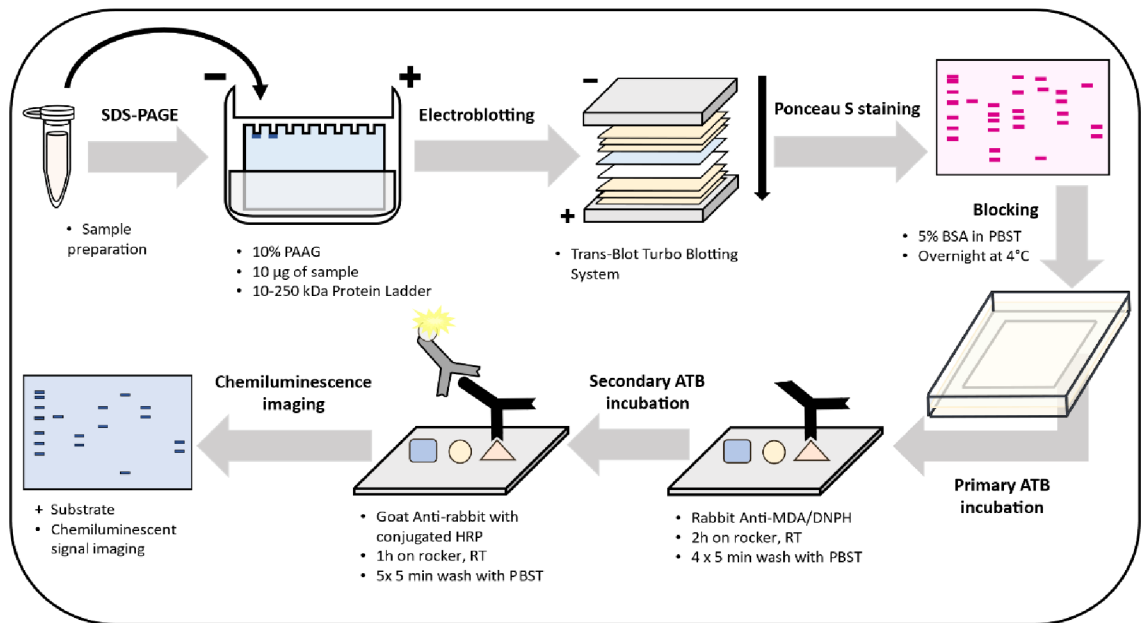
Figure 6: Flowchart depicting the workflow of western blot protocol from sample preparation to imaging.

4   Results and Discussion

4.1   Imaging of ultra-weak photon emission

Highly sensitive CCD camera VersArray 1300B was used for two-dimensional imaging of the ultra-weak photon emission emitted by biological samples (intact porcine ear/skin biopsies) spontaneously and after topical application of the selected treatment. The chemicals (Fenton's reagent and sodium ascorbate) when measured without the presence of skin sample were observed to induce UPE with an intensity comparable to that of the spontaneous emission of the biological sample, indicating no alteration to further measurements, as was observed in the previous study Prasad et al., (2018). To determine the ideal working concentration of the Fenton's reagent for the following experiments, a fixed concentration of $FeSO_4$ (250 µM) was mixed with varying concentrations of H_2O_2 (10 mM, 5 mM, and 2.5 mM), and the changes in UPE after the application to skin were measured (Fig. 7). Panel A of the Figure 7 shows the photograph of the prepared skin biopsies fixed to the experimental setup, panel B represents the spontaneous UPE (to demonstrate its variability within the sample set), and panel C depicts the UPE induced following the treatment application [0 mM (a), 2.5 mM (b), 5 mM (c), and 10 mM H_2O_2 (d)]. With higher concentration of oxidants, the photon count following 30 minutes of measurement enhanced. This observation confirms the role of Fenton's reagent as a substantial inducer of ROS-mediated UPE generation. Moreover, these findings indicate a direct correlation of UPE dependency on H_2O_2 concentration in the system. Fenton's reagent with the highest H_2O_2 concentration (10 mM) was therefore utilized in all subsequent measurements as seen in the Figure 8. The whole *ex-vivo* porcine ear was used for the UPE imaging in the Figure 8, where the left panel (8A) represents the spontaneous UPE, and the right panel (8B) shows the UPE measured after the application of the reagent. The graphs denoted by lowercase letters a, and b represent the photon intensity (given in relative units (r.u.) captured by the CCD camera at the corresponding pixels of the image marked by the white dotted line in the images 8A and 8B, respectively. The signal on the left to the treatment site (8B) also represented on the intensity graph (8b) (smaller peak) is the portion of skin to which the reagent diffused during the measurement, therefore, for analysis, only the data obtained from the direct treatment site (red circle) were considered. The intensity of the UPE observed showed apparent differences between the control (not treated); sample (8A, and a) that displayed no

enhancement, and the sample treated with 250 µM FeSO$_4$/10 mM H$_2$O$_2$ where the maximum intensity observed was~25 counts/pixel.
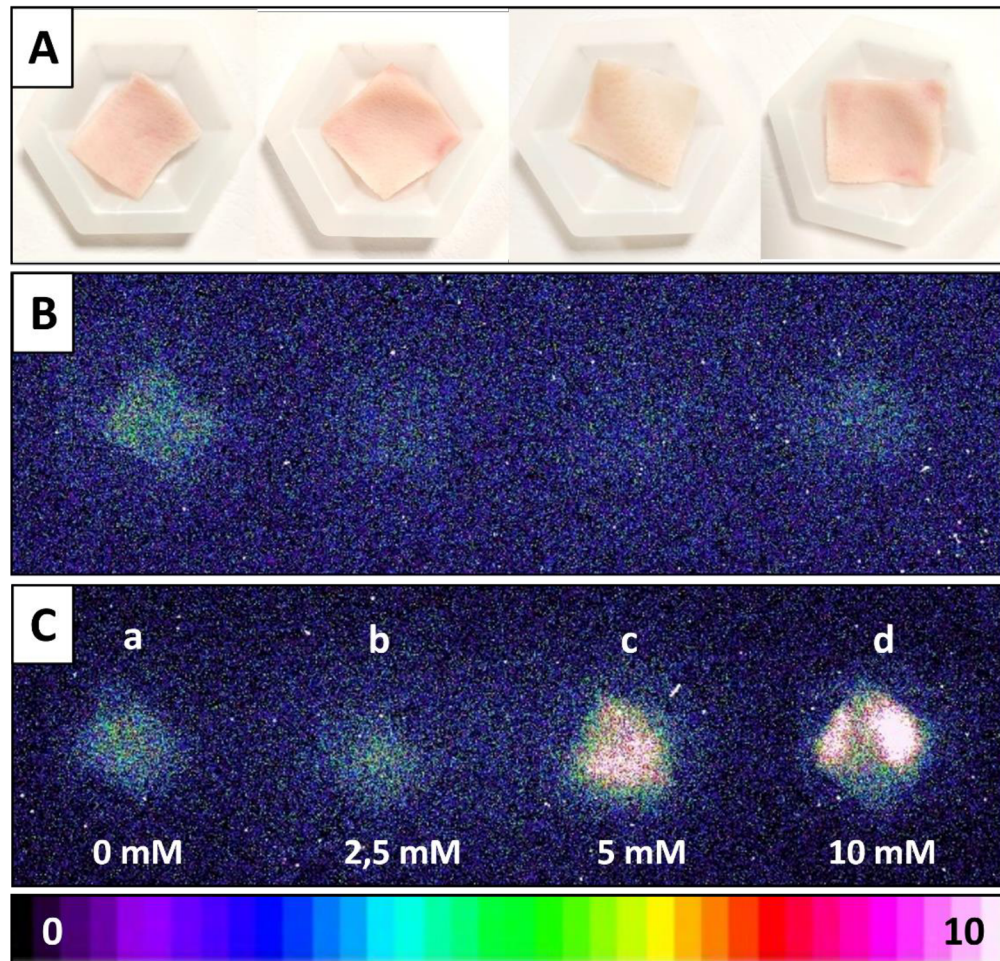

Figure 7: 2D photon emission imaging of skin biopsies with a highly sensitive CCD camera. Photographs of skin biopsies (A). Two-dimensional CCD camera images of spontaneous (B) and induced (C) ultra-weak photon emission from four pig skin biopsies. Increase in the UPE intensity in contrast with the control sample [(a) – no treatment] and induced by the topical application of Fenton's reagent containing 250 µM FeSO$_4$ and 2.5 mM (b), 5 mM (c), and 10 mM (d) H$_2$O$_2$. Scale represents photon counts per pixel.
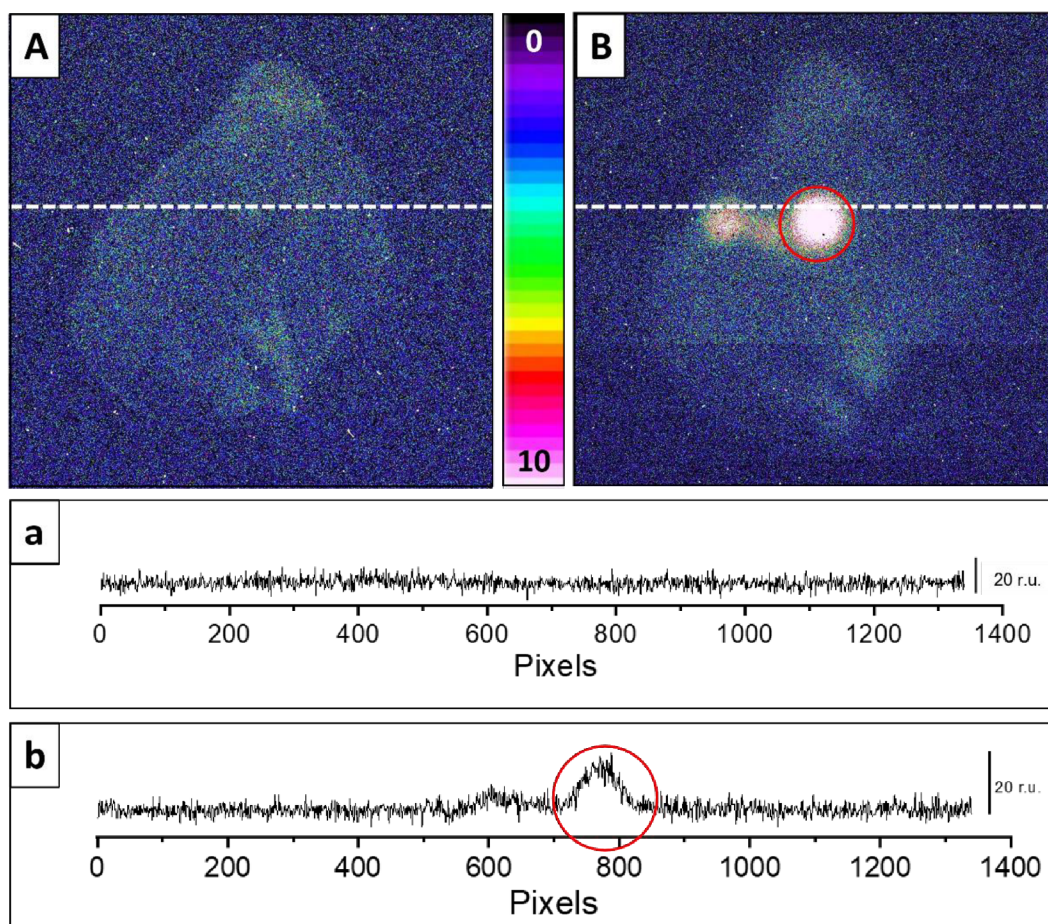
Figure 8: Two-dimensional CCD camera images of spontaneous (A) and induced (B) UPE from whole *ex-vivo* pig ear along with the corresponding intensity graphs (a and b respectively). The Fenton's reagent (250 µM FeSO$_4$ /10 mM H$_2$O$_2$) was topically applied to the treatment site denoted by the red circle (B and b) ~3 min preceding the measurement. Scale represents photon counts per pixel. The intensity graphs are a direct representation of the photon intensity observed in the area marked by white dashed line in the images. Y-axis on the graphs depicts the amount of pixel counts accumulated after 30 min, and the X-axis shows the pixel of the image.

4.2 Singlet oxygen and ^{3}C=O* contribution to UPE formation

To confirm the contribution of ROS in the detected Fenton's reagent stimulated photon emission, sodium ascorbate as one of the well-known scavengers of ^{1}O$_2$ (Halliwell & Gutteridge, 1990; Yadav et al., 2015) was utilized (Fig. 9). A solution of 10 mM sodium ascorbate was applied topically to the treatment site (indicated by yellow circle) 10 minutes before the Fenton's reagent (250 µM FeSO$_4$/10 mM H$_2$O$_2$) to ensure adequate tissue saturation. Additionally, to eliminate possible errors and guarantee the same conditions during the data collection and analysis, Fenton's reagent with the same concentration was applied (red circle) near the sodium ascorbate pre-treated site for direct

comparison. Two-dimensional CCD camera image of the whole *ex-vivo* pig ear depicts the observed intensity of induced UPE on the treatment sites (Fig. 9A). The grey dashed rectangle represents the area of the original image that had been cropped and magnified (Fig. 9B). The intensity graph (Fig. 9b) linked to images 9A and B was constructed directly from the area indicated by the white dashed line. The results reflect the notable difference in the emission intensity between the two treatment sites. Where Fenton's reagent led to the expected accumulation of photon counts/pixel exceeding ~25 (as seen in previous figures), the effect of the scavenger generated a photon count/pixel only slightly higher than that of the spontaneous UPE. The almost complete suppression of the signal due to the sodium ascorbate application indicates that the involvement of $^1O_2$ photon emission in the overall ultra-weak photon emission is substantial. This can be supported by the fact that the excitation energy in an oxygen-rich environment, can be transferred via triplet-singlet energy transfer from $^3C=O^*$, leading to the formation of $^1O_2$. If two $^1O_2$ collide, the resulting photon emission (referred to as dimol emission) is known to be in the red region of the spectrum (634 and 703 nm) (Pospíšil et al., 2019). Following the indication of $^3C=O^*$ being one of the primary sources of the oxidative stress induced UPE, an interference filter 644 (340-540 nm), that allowed for the passage of photons mostly limited to those emitted within the range attributed to $^3C=O^*$ (350-550 nm), was mounted in front of the objective lens. After using the filter, the intensity of the induced UPE captured in the picture C of Fig. 9 and the corresponding intensity graph (Fig. 9c); both still showed a partial signal of ~10 counts/pixel. These results suggest that the $^3C=O^*$ could be another type of ROS making up a considerable portion of the ultra-weak photon emission from the skin under oxidative stress.
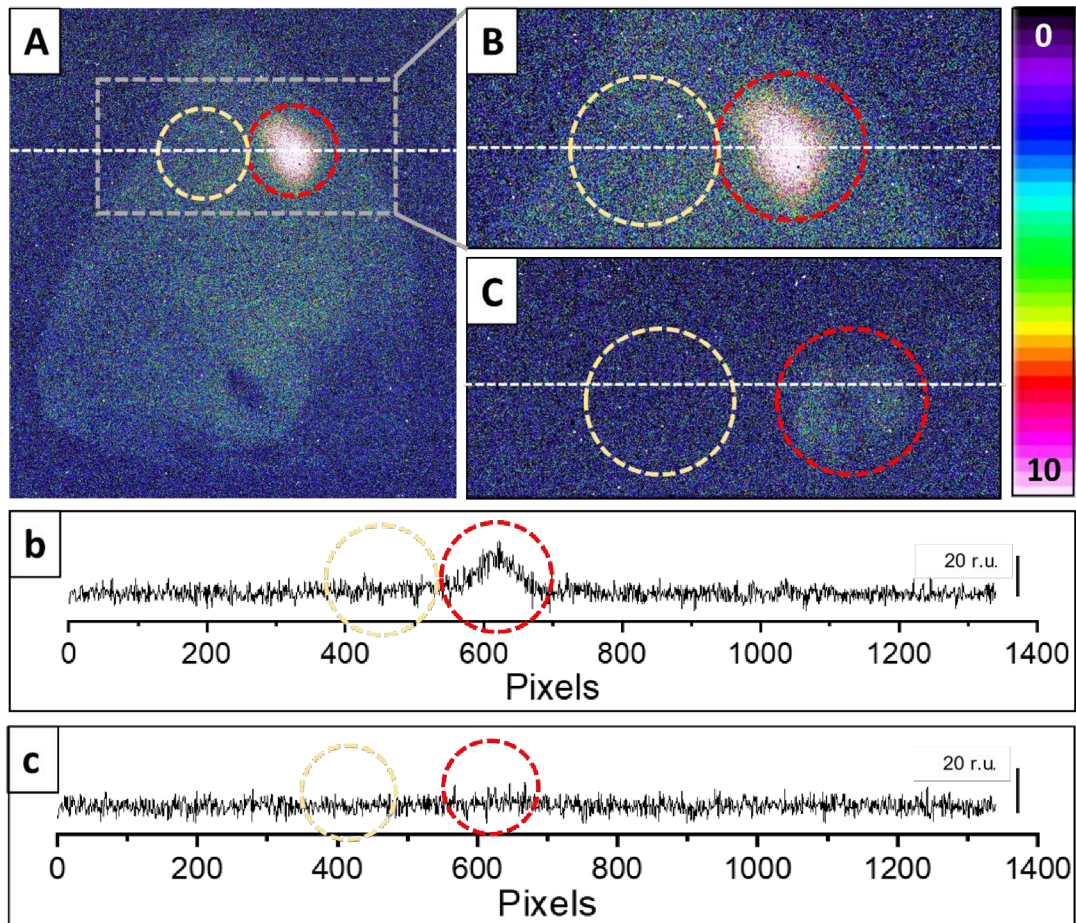
Figure 9: 2D-imaging of Fenton's reagent (250 µM FeSO$_4$/10 mM H$_2$O$_2$) induced UPE from whole porcine ear (A) in the presence (yellow circle) and absence (red circle) of sodium ascorbate (10 mM). The exogenous application of sodium ascorbate was done 10 min prior to the application of Fenton's reagent. Images (B) and (C) were cropped and magnified from the original images showing the application sites. Interference filter type 644 (340-540 nm) was mounted in front of the objective lens and a 2D image of Fenton's reagent induced UPE in the presence and absence of sodium ascorbate was captured. Intensity graphs (b) and (c) were constructed from the area indicated by white dotted line in the images (B) and (C) respectively. Y-axis on the graphs depicts the amount of pixel counts accumulated after 30 min, and the X-axis shows the pixel of the image.

4.3 Protein modifications under induced oxidative stress

By tipping the body's delicate intrinsic balance in favor of amplified ROS production, the number of oxidative radical reactions increases, causing the biomolecules (lipids, proteins, DNA, and carbohydrates) to be modified (Sies, 2018). In the present study, immunoblotting technique was used to study the ROS-mediated protein alterations (protein carboxylation and carbonyl formation) with anti-MDA and anti-DNP antibodies respectively. After preparing the pig skin lysates, and introducing the treatment (10 mM H_2O_2, or Fenton's reagent (250 μM $FeSO_4$/10 mM H_2O_2), the treated and non-treated samples were separated using SDS PAGE. MDA is a known marker of oxidative stress; It is formed as one of the products of lipid peroxidation when the produced ROS degrades polyunsaturated fatty acids (primarily located in cell membranes) through a chain of reactions (Sadrzadeh et al., 1984; Halliwell et al., 1993) (Fig. 11). This product can then react with amino acid residues (mainly Lys, Arg, His, and Cys) and form adducts with proteins (Chio et al., 1969; Chio & Tappel, 1969; Esterbauer et al., 1991). The MDA-protein adducts (MDA-modified proteins) were detected with anti-MDA antibody, and noticeable bands were observed around 15 kDa, 45 kDa, 50 kDa, 65 kDa, 130 kDa, and 250 kDa (Fig. 10A). Additionally, the 65 kDa and 130 kDa band density was found to be higher/comparable in case of H_2O_2 and Fenton's reagent respectively in comparison to the control protein band density, indicating that the lipid peroxidation product formation was enhanced via increased ROS production. The densitograms were constructed for both lanes displaying the differences in the densities (Fig. 10B).
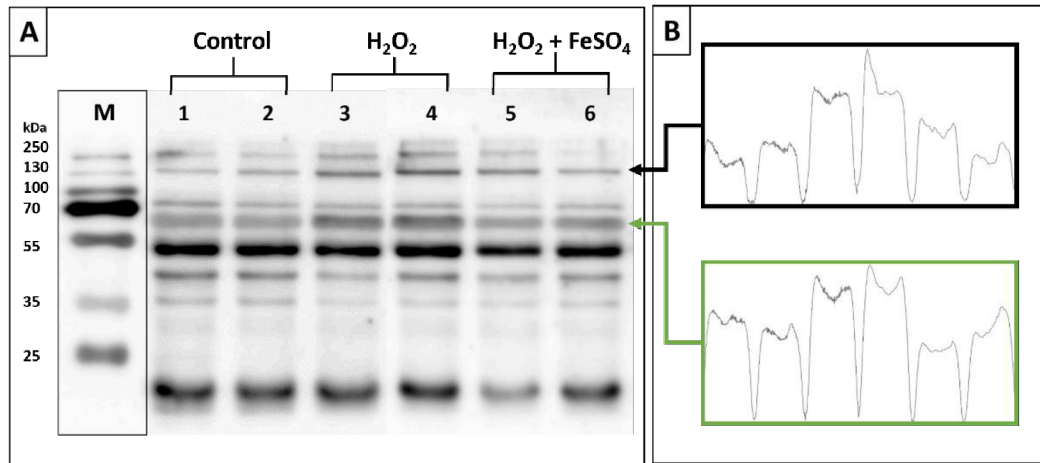
Figure 11: MDA-protein adducts identified in pig skin lysates (A). Control samples are shown in lanes 1-2, samples treated with H_2O_2 (10 mM) in lanes 3-4, and samples treated with Fenton's reagent (250 μM $FeSO_4$/10 mM H_2O_2) in lanes 5-6. Densitograms (protein band quantification) correspond to the lanes indicated by arrows and were constructed using ImageJ software.
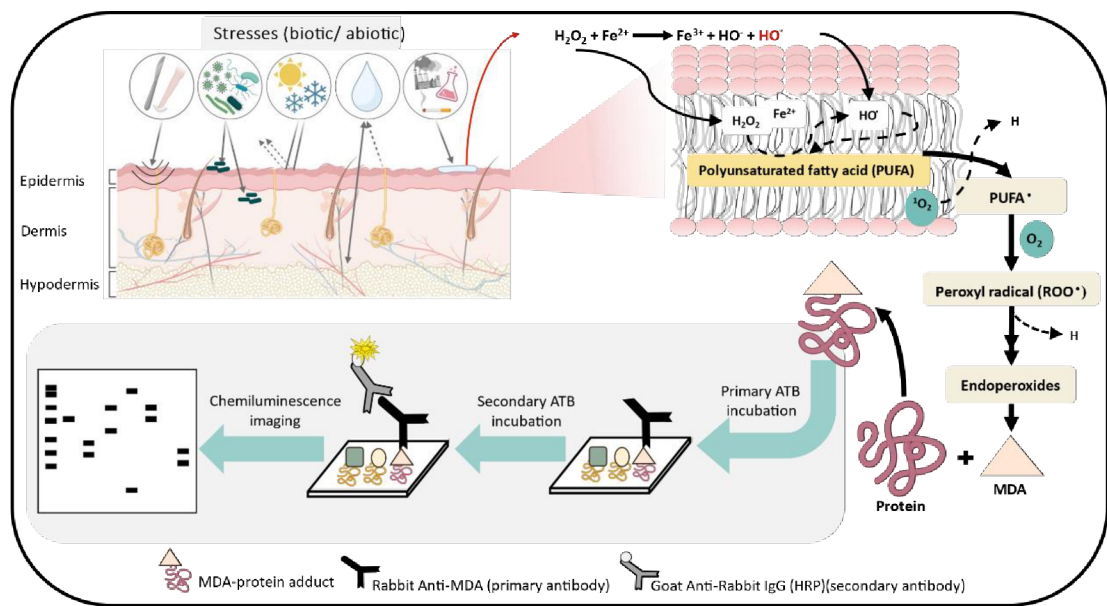

Figure 101: Scheme depicting the MDA-protein adduct formation resulting from chemically induced ROS generation and subsequent chain of oxidative radical reactions. Upper panel portrays various forms of environmental stresses that can promote ROS formation leading to lipid peroxidation (chain of oxidative radical reactions) with MDA as the end product. MDA can subsequently react with proteins and the adducts can be detected via immunoblotting techniques (lower panel).

The detection of protein carbonyl formation required a derivatization of samples preceding their separation through the SDS-PAGE as the carbonyls cannot be easily detected directly (Yan & Forster, 2011). The DNPH reacts with the carbonylated proteins present in the sample and produces 2,4- dinitrophenylhydrazone (DNP) group which eases the detection. In the current study, the protein-bound carbonyl in the pig skin lysates, both the non-treated (control), Fenton's reagent (250 µM $FeSO_4$/10 mM H_2O_2) treated, were detected via western blot analysis using anti-DNP antibody. Bands were detected at 250 kDa, 190 kDa, 120 kDa, 54 kDa, 35 kDa and 15 kDa mark (Fig. 12B). Panel A shows the total transferred protein content visible after Ponceau staining (Fig. 13A). The 35 kDa and 15 kDa bands show the most notable differences in density. Where Fenton's reagent treated samples showed comparable or even lower signal than the control samples, the sodium ascorbate treated samples produced bands with the highest density. The lower density of the bands in Fenton's reagent samples could be attributed to the proteins being degraded/modified in a manner different to the carbonylated protein formation due to the induced ROS generation, as well as the fact that the ELFO and western blotting can only measure the protein-bound carbonyls. Protein oxidation has been shown to generate not only protein-bound, but also low-molecular-mass carbonyls; therefore, the yield of protein-derived carbonyls could be higher without it reflecting on the western blot results (Headlam & Davies, 2004) (Fig.13). Figure 13 depicts the mechanism of protein carbonyl formation and detection via immunoblotting. DNPH blotting analysis with H_2O_2 was also conducted with results shown in the Prasad et al., (2023) in Figure 6 attached as part of the appendices.
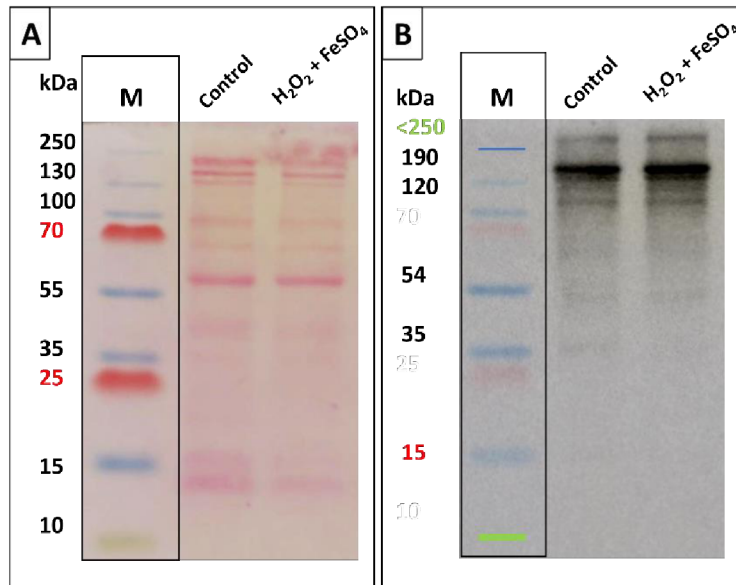
Figure 132: DNP-carbonyl derivates identified in pig skin lysates using anti-DNP rabbit antibody (B). Total transferred protein content was visualized through Ponceau staining (A). Lane following the molecular marker (right to left) contains non-treated (control) sample and the Fenton's reagent treated (250 µM FeSO$_4$/10 mM H$_2$O$_2$) sample is in the second lane.
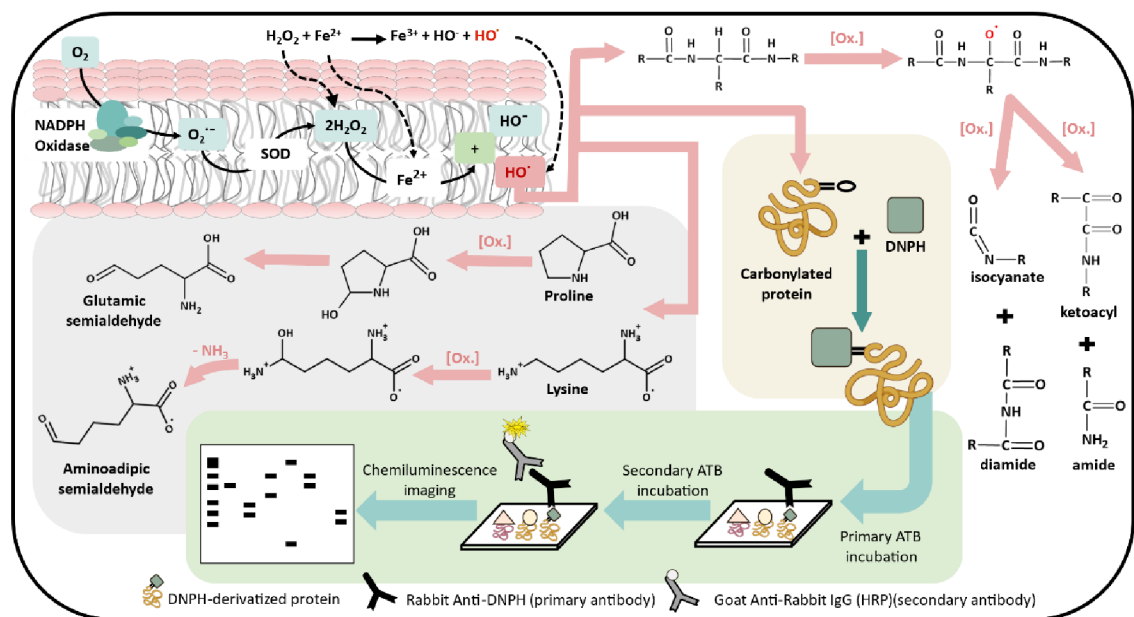

Figure 12: Scheme portraying the possible pathways of protein oxidation resulting in protein-bound and low-molecular-mass carbonyl formation. The lower panel shows the protein-bound carbonyl detection via DNP-protein adduct formation and western blot detection using anti-DNP antibody.

5 Conclusions

The skin is the largest organ of the human body and plays a crucial role in numerous bodily processes and functions. One of which is the protection against environmental stressors like oxidative stress. Excess ROS production has been reported to be a factor in ageing, as well as many diseases (mainly age-related). For research purposes, model systems that share attributes integral to the research purpose (morphology, biochemical composition, etc.), pig skin – in the current study – are oftentimes preferred to using human skin due to being ethically and economically more advantageous. The spectral analysis of the two-dimensional spatiotemporal CCD imaging confirmed the participation of singlet oxygen dimol emission and triplet excited carbonyls as considerable contributors to oxidatively induced (H_2O_2/Fenton's reagent) UPE formation in the skin. Blot analysis confirmed the presence of oxidatively modified protein adducts and showed differences in the band density from selected protein bands of the non-treated and H_2O_2 treated skin tissues. The results obtained in the present study aid in the further identification of specific protein targets along with the excited species directly involved/ contributing to the oxidative damage in skin and could serve as the base for developing/ improving the techniques used to distinguish the physiological and pathological state of an organism under oxidative stress. Additionally, Spatiotemporal CCD camera imaging is presented as a powerful non-invasive detection technique, that could after further technical advancement have the potential to be used in diverse research fields and/or clinical trials.

6   References

Arnér, E. S. J., & Holmgren, A. (2000). Physiological functions of thioredoxin and thioredoxin reductase. *European Journal of Biochemistry*, *267*(20), 6102–6109. https://doi.org/10.1046/J.1432-1327.2000.01701.X

Avon, S. L., & Wood, R. E. (2005). Porcine skin as an in-vivo model for ageing of human bite marks. *Journal of Forensic Odonto-Stomatology*, *23*(2), 30–39.

Bae, Y. S., Oh, H., Rhee, S. G., & Yoo, Y. Do. (2011). Regulation of reactive oxygen species generation in cell signaling. *Molecules and Cells*, *32*(6), 491–509. https://doi.org/10.1007/S10059-011-0276-3

Baron, J. M., Höller, D., Schiffer, R., Frankenberg, S., Neis, M., Merk, H. F., & Jugert, F. K. (2001). Expression of multiple cytochrome p450 enzymes and multidrug resistance-associated transport proteins in human skin keratinocytes. *The Journal of Investigative Dermatology*, *116*(4), 541–548. https://doi.org/10.1046/J.1523-1747.2001.01298.X

Bizzozero, O. A. (2009). Protein Carbonylation in Neurodegenerative and Demyelinating CNS Diseases. *Handbook of Neurochemistry and Molecular Neurobiology*, 543–562. https://doi.org/10.1007/978-0-387-30375-8_23

Block, K., Gorin, Y., & Abboud, H. E. (2009). Subcellular localization of Nox4 and regulation in diabetes. *Proceedings of the National Academy of Sciences of the United States of America*, *106*(34), 14385–14390. https://doi.org/10.1073/PNAS.0906805106

Bollineni, R. C., Hoffmann, R., & Fedorova, M. (2011). Identification of protein carbonylation sites by two-dimensional liquid chromatography in combination with MALDI- and ESI-MS. *Journal of Proteomics*, *74*(11), 2338–2350. https://doi.org/10.1016/J.JPROT.2011.07.002

Bouten, C., Oomens, C., Colin, D., & Bader, D. (2005). Skin model studies. In *Pressure Ulcer Research: Current and Future Perspectives* (pp. 263–285). Springer, Berlin, Heidelberg. https://doi.org/10.1007/3-540-28804-X_1

Buss, H., Chan, T. P., Sluis, K. B., Domigan, N. M., & Winterbourn, C. C. (1997). Protein carbonyl measurement by a sensitive ELISA method. *Free Radical Biology and Medicine*, *23*(3), 361–366. https://doi.org/10.1016/S0891-5849(97)00104-4

Chen, L., Hu, J. Y., & Wang, S. Q. (2012). The role of antioxidants in photoprotection: a critical review. *Journal of the American Academy of Dermatology*, *67*(5), 1013–1024. https://doi.org/10.1016/J.JAAD.2012.02.009

Chio, K. S., & Tappel, A. L. (1969). Synthesis and characterization of the fluorescent products derived from malonaldehyde and amino acids. *Biochemistry*, *8*(7), 2821–2827. https://doi.org/10.1021/BI00835A019

Chio, K. S., Tappel, A. L., Crawford, D. L., Yu, T. C., Sinnhuber, R. O., Feldmann, K., Daltrozzo, E., Scheibe, G., Fischer, E., Freí, Y., Heinert, D., Martell, A. E., Hendley, D. D., Mildvan, A. S., Reporter, M. G., Strehler, B. L., Hydén, H., Lindstrom, B., Kwon, T. W., … Skoldinov, A. P. (1969). Inactivation of Ribonuclease and Other Enzymes by Peroxidizing Lipids and by Malonaldehyde. *Biochemistry*, *8*(7), 2827–2832. https://doi.org/10.1021/BI00835A020

Chiu, T., & Burd, A. (2005). "Xenograft" dressing in the treatment of burns. *Clinics in Dermatology*, *23*(4), 419–423. https://doi.org/10.1016/J.CLINDERMATOL.2004.07.027

Chiumiento, L., & Bruschi, F. (2009). Enzymatic antioxidant systems in helminth parasites. *Parasitology Research*, *105*(3), 593–603. https://doi.org/10.1007/S00436-009-1483-0/FIGURES/4

Cifra, M., & Pospíšil, P. (2014). Ultra-weak photon emission from biological samples:

Definition, mechanisms, properties, detection and applications. *Journal of Photochemistry and Photobiology B: Biology, 139,* 2–10. https://doi.org/10.1016/j.jphotobiol.2014.02.009

Clark, M., & Tilman, D. (2017). Comparative analysis of environmental impacts of agricultural production systems, agricultural input efficiency, and food choice. *Environmental Research Letters, 12*(6). https://doi.org/10.1088/1748-9326/AA6CD5

Dahlgren, C., Karlsson, A., & Bylund, J. (2007). Measurement of respiratory burst products generated by professional phagocytes. *Methods in Molecular Biology (Clifton, N.J.), 412,* 349–363. https://doi.org/10.1007/978-1-59745-467-4_23

Dalle-Donne, I., Rossi, R., Giustarini, D., Milzani, A., & Colombo, R. (2003). Protein carbonyl groups as biomarkers of oxidative stress. *Clinica Chimica Acta; International Journal of Clinical Chemistry, 329*(1–2), 23–38. https://doi.org/10.1016/S0009-8981(03)00003-2

Debeer, S., Le Luduec, J. B., Kaiserlian, D., Laurent, P., Nicolas, J. F., Dubois, B., & Kanitakis, J. (2013). Comparative histology and immunohistochemistry of porcine versus human skin. *European Journal of Dermatology, 23*(4), 456–466. https://doi.org/10.1684/EJD.2013.2060

Dobrakowski, M., Kasperczyk, A., Pawlas, N., Birkner, E., Hudziec, E., Chwalińska, E., & Kasperczyk, S. (2016). Association between subchronic and chronic lead exposure and levels of antioxidants and chemokines. *International Archives of Occupational and Environmental Health, 89*(7), 1077. https://doi.org/10.1007/S00420-016-1144-4

Dyring-Andersen, B., Løvendorf, M. B., Coscia, F., Santos, A., Møller, L. B. P., Colaço, A. R., Niu, L., Bzorek, M., Doll, S., Andersen, J. L., Clark, R. A., Skov, L., Teunissen, M. B. M., & Mann, M. (2020). Spatially and cell-type resolved quantitative proteomic atlas of healthy human skin. *Nature Communications, 11*(1), 1–14. https://doi.org/10.1038/s41467-020-19383-8

Elias, P. M. (2007). The skin barrier as an innate immune element. *Seminars in Immunopathology, 29*(1), 3–14. https://doi.org/10.1007/S00281-007-0060-9/TABLES/7

Ericsson, A. C., Crim, M. J., & Franklin, C. L. (2013). A Brief History of Animal Modeling. *Missouri Medicine, 110*(3), 201.

Esterbauer, H, & Hpuhl, G. (1993). Lipid peroxidation and its role in atherosclerosis. *British Medical Bulletin, 49*(3), 566–576.

Esterbauer, Hermann, Schaur, R. J., & Zollner, H. (1991). Chemistry and biochemistry of 4-hydroxynonenal, malonaldehyde and related aldehydes. *Free Radical Biology & Medicine, 11*(1), 81–128. https://doi.org/10.1016/0891-5849(91)90192-6

Fedorova, M. (2017). Diversity of Protein Carbonylation Pathways. In J. Ros (Ed.), *Protein Carbonylation: Principles, Analysis, and Biological Implications* (pp. 48–82). John Wiley & Sons, Ltd. https://doi.org/10.1002/9781119374947.CH3

Fransen, M., Nordgren, M., Wang, B., & Apanasets, O. (2012). Role of peroxisomes in ROS/RNS-metabolism: implications for human disease. *Biochimica et Biophysica Acta, 1822*(9), 1363–1373. https://doi.org/10.1016/J.BBADIS.2011.12.001

Fruehauf, J. P., & Trapp, V. (2008). Reactive oxygen species: an Achilles' heel of melanoma? *Expert Review of Anticancer Therapy, 8*(11), 1751–1757. https://doi.org/10.1586/14737140.8.11.1751

Gambhir, J. K., Lali, P., & Jain, A. K. (1997). Correlation between blood antioxidant levels and lipid peroxidation in rheumatoid arthritis. *Clinical Biochemistry, 30*(4), 351–355. https://doi.org/10.1016/S0009-9120(96)00007-0

Gasparovic, A. C., Jaganjac, M., Mihaljevic, B., Sunjic, S. B., & Zarkovic, N. (2013). Assays for the measurement of lipid peroxidation. *Methods in Molecular Biology*, *965*, 283–293. https://doi.org/10.1007/978-1-62703-239-1_19

Gorsky, L. D., Koop, D. R., & Coon, M. J. (1984). On the stoichiometry of the oxidase and monooxygenase reactions catalyzed by liver microsomal cytochrome P-450. Products of oxygen reduction. *Journal of Biological Chemistry*, *259*(11), 6812–6817. https://doi.org/10.1016/S0021-9258(17)39800-9

Guéraud, F., Atalay, M., Bresgen, N., Cipak, A., Eckl, P. M., Huc, L., Jouanin, I., Siems, W., & Uchida, K. (2010). Chemistry and biochemistry of lipid peroxidation products. *Free Radical Research*, *44*(10), 1098–1124. https://doi.org/10.3109/10715762.2010.498477

Gupta, P., Lakes, A., & Dziubla, T. (2016). A Free Radical Primer. In *Oxidative Stress and Biomaterials* (pp. 1–34). Elsevier Inc.

Halliwell, B., Chirico, S., Crawford, M. A., Bjerve, K. S., & Gey, K. F. (1993). Lipid peroxidation: Its mechanism, measurement, and significance. *American Journal of Clinical Nutrition*, *57*(5 SUPPL.). https://doi.org/10.1093/AJCN/57.5.715S

Halliwell, Barry, Clement, M. V., & Long, L. H. (2000). Hydrogen peroxide in the human body. *FEBS Letters*, *486*(1), 10–13. https://doi.org/10.1016/S0014-5793(00)02197-9

Halliwell, Barry, & Gutteridge, J. M. C. (1990). [1] Role of free radicals and catalytic metal ions in human disease: An overview. *Methods in Enzymology*, *186*(C), 1–85. https://doi.org/10.1016/0076-6879(90)86093-B

Halliwell, Barry, & Gutteridge, J. M. C. (2015). Free Radicals in Biology and Medicine. *Free Radicals in Biology and Medicine*. https://doi.org/10.1093/ACPROF:OSO/9780198717478.001.0001

Hammond, S. A., Tsonis, C., Sellins, K., Rushlow, K., Scharton-Kersten, T., Colditz, I., & Glenn, G. M. (2000). Transcutaneous immunization of domestic animals: opportunities and challenges. *Advanced Drug Delivery Reviews*, *43*(1), 45–55. https://doi.org/10.1016/S0169-409X(00)00076-4

Hawkins, C. L., & Davies, M. J. (2019). Detection, identification, and quantification of oxidative protein modifications. *The Journal of Biological Chemistry*, *294*(51), 19683. https://doi.org/10.1074/JBC.REV119.006217

Headlam, H. A., & Davies, M. J. (2004). Markers of protein oxidation: Different oxidants give rise to variable yields of bound and released carbonyl products. *Free Radical Biology and Medicine*, *36*(9), 1175–1184. https://doi.org/10.1016/j.freeradbiomed.2004.02.017

Hecker, M., & Wagner, A. H. (2018). Role of protein carbonylation in diabetes. *Journal of Inherited Metabolic Disease*, *41*(1), 29–38. https://doi.org/10.1007/S10545-017-0104-9

Heinrich, W., Lange, P. M., Stirtz, T., Iancu, C., & Heidemann, E. (1971). Isolation and characterization of the large cyanogen bromide peptides from the alpha1- and alpha2-chains of pig skin collagen. *FEBS Letters*, *16*(1), 63–67. https://doi.org/10.1016/0014-5793(71)80687-7

Höhn, A., König, J., & Grune, T. (2013). Protein oxidation in aging and the removal of oxidized proteins. *Journal of Proteomics*, *92*, 132–159. https://doi.org/10.1016/J.JPROT.2013.01.004

Holbrook, K. A. (1989). Biologic Structure and Function: Perspectives on Morphologic Approaches to the Study of the Granular Layer Keratinocyte. *Journal of Investigative Dermatology*, *92*(4), S84–S104. https://doi.org/10.1038/JID.1989.36

Huber, K. R., Sridhar, R., Griffith, E. H., Amma, E. L., & Roberts, J. (1987).

Superoxide dismutase-like activities of copper(II) complexes tested in serum. *Biochimica et Biophysica Acta (BBA)/Protein Structure and Molecular*, *915*(2), 267–276. https://doi.org/10.1016/0167-4838(87)90309-8

Jeon, S., Djian, P., & Green, H. (1998). Inability of keratinocytes lacking their specific transglutaminase to form cross-linked envelopes: Absence of envelopes as a simple diagnostic test for lamellar ichthyosis. *Proceedings of the National Academy of Sciences of the United States of America*, *95*(2), 687–690. https://doi.org/10.1073/PNAS.95.2.687

Ji, H., & Li, X. K. (2016). Oxidative Stress in Atopic Dermatitis. *Oxidative Medicine and Cellular Longevity*, *2016*(Figure 1). https://doi.org/10.1155/2016/2721469

Karges, J. (2022). Clinical Development of Metal Complexes as Photosensitizers for Photodynamic Therapy of Cancer. *Angewandte Chemie International Edition*, *61*(5), e202112236. https://doi.org/10.1002/ANIE.202112236

Kehm, R., Baldensperger, T., Raupbach, J., & Höhn, A. (2021). Protein oxidation - Formation mechanisms, detection and relevance as biomarkers in human diseases. *Redox Biology*, *42*, 101901. https://doi.org/10.1016/J.REDOX.2021.101901

Klaunig, J. E., Kamendulis, L. M., & Hocevar, B. A. (2010). Oxidative stress and oxidative damage in carcinogenesis. *Toxicologic Pathology*, *38*(1), 96–109. https://doi.org/10.1177/0192623309356453

Korbecki, J., Baranowska-Bosiacka, I., Gutowska, I., & Chlubek, D. (2013). The effect of reactive oxygen species on the synthesis of prostanoids from arachidonic acid. *Journal of Physiology and Pharmacology : An Official Journal of the Polish Physiological Society*, *64*(4), 409–421.

Levine, R. L., Garland, D., Oliver, C. N., Amici, A., Climent, I., Lenz, A. G., Ahn, B. W., Shaltiel, S., & Stadtman, E. R. (1990). Determination of carbonyl content in oxidatively modified proteins. *Methods in Enzymology*, *186*(C), 464–478. https://doi.org/10.1016/0076-6879(90)86141-H

Marrocco, I., Altieri, F., & Peluso, I. (2017). Measurement and Clinical Significance of Biomarkers of Oxidative Stress in Humans. *Oxidative Medicine and Cellular Longevity*, *2017*. https://doi.org/10.1155/2017/6501046

Martin, K. R., & Barrett, J. C. (2002). Reactive oxygen species as double-edged swords in cellular processes: Low-dose cell signaling versus high-dose toxicity. *Human and Experimental Toxicology*, *21*(2), 71–75. https://doi.org/10.1191/0960327102ht213oa

Masutin, V., Kersch, C., & Schmitz-Spanke, S. (2022). A systematic review: metabolomics-based identification of altered metabolites and pathways in the skin caused by internal and external factors. *Experimental Dermatology*. https://doi.org/10.1111/EXD.14529

Meurens, F., Summerfield, A., Nauwynck, H., Saif, L., & Gerdts, V. (2012). The pig: A model for human infectious diseases. *Trends in Microbiology*, *20*(1), 50–57. https://doi.org/10.1016/J.TIM.2011.11.002

Meyer, W., Schwarz, R., & Neurand, K. (1978). The skin of domestic mammals as a model for the human skin, with special reference to the domestic pig. *Current Problems in Dermatology*, *7*, 39–52. https://doi.org/10.1159/000401274

Morgan, P. E., Sturgess, A. D., Hennessy, A., & Davies, M. J. (2007). Serum protein oxidation and apolipoprotein CIII levels in people with systemic lupus erythematosus with and without nephritis. *Free Radical Research*, *41*(12), 1301–1312. https://doi.org/10.1080/10715760701684809

Naskalski, J. W., & Bartosz, G. (2001). Oxidative modifications of protein structures. *Advances in Clinical Chemistry*, *35*, 161–253. https://doi.org/10.1016/S0065-

2423(01)35017-5

Niedernhofer, L. J., Bohr, V. A., Sander, M., & Kraemer, K. H. (2011). Xeroderma pigmentosum and other diseases of human premature aging and DNA repair: molecules to patients. *Mechanisms of Ageing and Development*, *132*(6–7), 340–347. https://doi.org/10.1016/J.MAD.2011.06.004

Ohkawa, H., Ohishi, N., & Yagi, K. (1979). Assay for lipid peroxides in animal tissues by thiobarbituric acid reaction. *Analytical Biochemistry*, *95*(2), 351–358. https://doi.org/10.1016/0003-2697(79)90738-3

Oliver, C. N., Levine, R. L., & Stadtman, E. R. (1987). A Role of Mixed-Function Oxidation Reactions in the Accumulation of Altered Enzyme Forms During Aging. *Journal of the American Geriatrics Society*, *35*(10), 947–956. https://doi.org/10.1111/j.1532-5415.1987.tb02297.x

Pisoschi, A. M., Pop, A., Iordache, F., Stanca, L., Predoi, G., & Serban, A. I. (2021). Oxidative stress mitigation by antioxidants - An overview on their chemistry and influences on health status. *European Journal of Medicinal Chemistry*, *209*, 112891. https://doi.org/10.1016/J.EJMECH.2020.112891

Poli, G., Dianzani, M. U., Cheeseman, K. H., Slater, T. F., Lang$, J., & Esterbauert, H. (1985). Separation and characterization of the aldehydic products of lipid peroxidation stimulated by carbon tetrachloride or ADP-iron in isolated rat hepatocytes and rat liver microsomal suspensions. *Biochem. J*, *227*, 629–638.

Poljšak, B., & Dahmane, R. (2012). Free radicals and extrinsic skin aging. *Dermatology Research and Practice*, *2012*. https://doi.org/10.1155/2012/135206

Pospíšil, P., Prasad, A., & Rác, M. (2019). Mechanism of the formation of electronically excited species by oxidative metabolic processes: Role of reactive oxygen species. *Biomolecules*, *9*(7). https://doi.org/10.3390/biom9070258

Prasad, A., Balukova, A., & Pospíšil, P. (2018). Triplet Excited Carbonyls and Singlet Oxygen Formation During Oxidative Radical Reaction in Skin. *Frontiers in Physiology*, *0*(AUG), 1109. https://doi.org/10.3389/FPHYS.2018.01109

Prasad, A., Duchová, H., Manoharan, R. R., Rathi, D., & Pospíšil, P. (2023). Imaging and Characterization of Oxidative Protein Modifications in Skin. *International Journal of Molecular Sciences*, *24*(4), 3981. https://doi.org/10.3390/IJMS24043981/S1

Prasad, A., & Pospišil, P. (2011). Two-dimensional imaging of spontaneous ultra-weak photon emission from the human skin: Role of reactive oxygen species. *Journal of Biophotonics*, *4*(11–12), 840–849. https://doi.org/10.1002/jbio.201100073

Prasad, A., & Pospíšil, P. (2013). Towards the two-dimensional imaging of spontaneous ultra-weak photon emission from microbial, plant and animal cells. *Scientific Reports*, *3*. https://doi.org/10.1038/SREP01211

Proksch, E., Brandner, J. M., & Jensen, J.-M. (2008). The skin: an indispensable barrier. *Experimental Dermatology*, *17*, 1063–1072. https://doi.org/10.1111/j.1600-0625.2008.00786.x

Rastogi, A., & Pospíšil, P. (2011). Spontaneous ultraweak photon emission imaging of oxidative metabolic processes in human skin: effect of molecular oxygen and antioxidant defense system. *Journal of Biomedical Optics*, *16*(9), 096005. https://doi.org/10.1117/1.3616135

Rifkind, J. M., Mohanty, J. G., & Nagababu, E. (2015). The pathophysiology of extracellular hemoglobin associated with enhanced oxidative reactions. *Frontiers in Physiology*, *6*(JAN), 500. https://doi.org/10.3389/FPHYS.2014.00500/BIBTEX

Rinnerthaler, M., Bischof, J., Streubel, M. K., Trost, A., & Richter, K. (2015). Oxidative Stress in Aging Human Skin. *Biomolecules*, *5*(2), 545.

https://doi.org/10.3390/BIOM5020545

Rinnerthaler, M., Büttner, S., Laun, P., Heeren, G., Felder, T. K., Klinger, H., Weinberger, M., Stolze, K., Grousl, T., Hasek, J., Benada, O., Frydlova, I., Klocker, A., Simon-Nobbe, B., Jansko, B., Breitenbach-Koller, H., Eisenberg, T., Gourlay, C. W., Madeo, F., … Breitenbach, M. (2012). Yno1p/Aim14p, a NADPH-oxidase ortholog, controls extramitochondrial reactive oxygen species generation, apoptosis, and actin cable formation in yeast. *Proceedings of the National Academy of Sciences of the United States of America*, *109*(22), 8658–8663. https://doi.org/10.1073/PNAS.1201629109

Rinnerthaler, M., Duschl, J., Steinbacher, P., Salzmann, M., Bischof, J., Schuller, M., Wimmer, H., Peer, T., Bauer, J. W., & Richter, K. (2013). Age-related changes in the composition of the cornified envelope in human skin. *Experimental Dermatology*, *22*(5), 329–335. https://doi.org/10.1111/EXD.12135

Roy, S., Khanna, S., Nallu, K., Hunt, T. K., & Sen, C. K. (2006). Dermal wound healing is subject to redox control. *Molecular Therapy : The Journal of the American Society of Gene Therapy*, *13*(1), 211–220. https://doi.org/10.1016/J.YMTHE.2005.07.684

Rushmer, R. F., Buettner, K. J. K., Short, J. M., & Odland, G. F. (1996). The Skin. *Science*, *154*(3747), 343–348.

Sadrzadeh, S. M. H., Graf, E., Panter, S. S., Hallaway, P. E., & Eaton, J. W. (1984). Hemoglobin. A biologic Fenton reagent. *Journal of Biological Chemistry*, *259*(23), 14354–14356. https://doi.org/10.1016/s0021-9258(17)42604-4

Sandby-Møller, J., Poulsen, T., & Wulf, H. C. (2003). Epidermal Thickness at Different Body Sites: Relationship to Age, Gender, Pigmentation, Blood Content, Skin Type and Smoking Habits. *Acta Dermato-Venereologica*, *83*(6), 410–413. https://doi.org/10.1080/00015550310015419

Sander, C. S., Chang, H., Salzmann, S., Müller, C. S. L., Ekanayake-Mudiyanselage, S., Elsner, P., & Thiele, J. J. (2002). Photoaging is associated with protein oxidation in human skin In Vivo. *Journal of Investigative Dermatology*, *118*(4), 618–625. https://doi.org/10.1046/j.1523-1747.2002.01708.x

Schneider, C., Porter, N. A., & Brash, A. R. (2008). *Routes to 4-Hydroxynonenal: Fundamental Issues in the Mechanisms of Lipid Peroxidation. 283*(23), 15539–15543. https://doi.org/10.1074/jbc.R800001200

Sen, C. K., & Roy, S. (2008). Redox signals in wound healing. *Biochimica et Biophysica Acta - General Subjects*, *1780*(11), 1348–1361. https://doi.org/10.1016/J.BBAGEN.2008.01.006

Sies, H. (2018). On the history of oxidative stress: Concept and some aspects of current development. *Current Opinion in Toxicology*, *7*, 122–126. https://doi.org/10.1016/J.COTOX.2018.01.002

Sorolla, M. A., Rodríguez-Colman, M. J., Tamarit, J., Ortega, Z., Lucas, J. J., Ferrer, I., Ros, J., & Cabiscol, E. (2010). Protein oxidation in Huntington disease affects energy production and vitamin B6 metabolism. *Free Radical Biology & Medicine*, *49*(4), 612–621. https://doi.org/10.1016/J.FREERADBIOMED.2010.05.016

Starcher, B., Aycock, R. L., & Hill, C. H. (2005). Multiple Roles for Elastic Fibers in the Skin. *The Journal of Histochemistry & Cytochemistry*, *53*(4), 431–443. https://doi.org/10.1369/jhc.4A6484.2005

Strong, C. D. G., Wertz, P. W., Wang, C., Yang, F., Meltzer, P. S., Andl, T., Millar, S. E., Ho, I. C., Pai, S. Y., & Segre, J. A. (2006). Lipid defect underlies selective skin barrier impairment of an epidermal-specific deletion of Gata-3. *Journal of Cell Biology*, *175*(4), 661–670. https://doi.org/10.1083/JCB.200605057

Sullivan, T. P., Eaglstein, W. H., Davis, S. C., & Mertz, P. (2001). THE PIG AS A MODEL FOR HUMAN WOUND HEALING. *Wound Repair and Regeneration*, *9*(2), 66–76. https://doi.org/10.1046/J.1524-475X.2001.00066.X

Summerfield, A., Meurens, F., & Ricklin, M. E. (2015). The immunology of the porcine skin and its value as a model for human skin. *Molecular Immunology*, *66*(1), 14–21. https://doi.org/10.1016/J.MOLIMM.2014.10.023

Tsiropoulou, S., & Touyz, R. M. (2017). Assessment of protein carbonylation and protein tyrosine phosphatase (PTP) oxidation in vascular smooth muscle cells (VSMCS) using immunoblotting approaches. *Methods in Molecular Biology*, *1614*, 31–46. https://doi.org/10.1007/978-1-4939-7030-8_3/COVER

Turrens, J. F. (2003). Mitochondrial formation of reactive oxygen species. *Journal of Physiology*, *552*(2), 335–344. https://doi.org/10.1113/JPHYSIOL.2003.049478

Wang, Y.-N., & Sanders, J. (2005). Skin Model Studies. In *The Aetiopathology of Pressure Ulcers: A Hierarchical Approach* (pp. 268–285). Springer Berlin Heidelberg. https://doi.org/10.1007/3-540-28804-X_1

Weber, S. U., Thiele, J. J., Cross, C. E., & Packer, L. (1999). Vitamin C, Uric Acid, and Glutathione Gradients in Murine Stratum Corneum and their Susceptibility to Ozone Exposure. *Journal of Investigative Dermatology*, *113*(6), 1128–1132. https://doi.org/10.1046/J.1523-1747.1999.00789.X

Winston, G. W., Feierman, D. E., & Cederbaum, A. I. (1984). The role of iron chelates in hydroxyl radical production by rat liver microsomes, NADPH-cytochrome P-450 reductase and xanthine oxidase. *Archives of Biochemistry and Biophysics*, *232*(1), 378–390. https://doi.org/10.1016/0003-9861(84)90553-8

Wu, W. S. (2006). The signaling mechanism of ROS in tumor progression. *Cancer Metastasis Reviews*, *25*(4), 695–705. https://doi.org/10.1007/S10555-006-9037-8

Wysocki, A. B. (1999). Skin anatomy, physiology, and pathophysiology. *The Nursing Clinics of North America*, *34*(4).

Xu, H., Zheng, Y.-W., Liu, Q., Liu, L.-P., Luo, F.-L., Hu-ChenZhou, Isoda, H., Ohkohchi, N., & Li, Y.-M. (2017). Reactive Oxygen Species in Skin Repair, Regeneration, Aging, and Inflammation. *Reactive Oxygen Species (ROS) in Living Cells*. https://doi.org/10.5772/INTECHOPEN.72747

Yadav, D., Prasad, A., Kruk, J., & Pospíšil, P. (2015). Correction: Evidence for the Involvement of Loosely Bound Plastosemiquinones in Superoxide Anion Radical Production in Photosystem II. *PLOS ONE*, *10*(6), e0130244. https://doi.org/10.1371/JOURNAL.PONE.0130244

Yan, L. J., & Forster, M. J. (2011). Chemical probes for analysis of carbonylated proteins: a review. *Journal of Chromatography. B, Analytical Technologies in the Biomedical and Life Sciences*, *879*(17–18), 1308–1315. https://doi.org/10.1016/J.JCHROMB.2010.08.004

Yengi, L. G., Xiang, Q., Pan, J., Scatina, J. A., Kao, J., Ball, S. E., Fruncillo, R., Ferron, G., & Wolf, C. R. (2003). Quantitation of cytochrome P450 mRNA levels in human skin. *Analytical Biochemistry*, *316*(1), 103–110. https://doi.org/10.1016/S0003-2697(03)00042-3

Zhang, J., Fu, Y., Yang, P., Liu, X., Li, Y., & Gu, Z. (2020). ROS Scavenging Biopolymers for Anti-Inflammatory Diseases: Classification and Formulation. *Advanced Materials Interfaces*, *7*(16), 2000632. https://doi.org/10.1002/ADMI.202000632

Zhang, Y., Dai, M., & Yuan, Z. (2018). Methods for the detection of reactive oxygen species. *Analytical Methods*, *10*(38), 4625–4638. https://doi.org/10.1039/C8AY01339J

Zhou, Z., Song, J., Nie, L., & Chen, X. (2016). Reactive Oxygen Species Generating Systems Meeting Challenges of Photodynamic Cancer Therapy. *Chemical Society Reviews*, *45*(23), 6597. https://doi.org/10.1039/C6CS00271D

7　List of Abbreviations

$^1O_2$	singlet oxygen
$^3C{=}O^{\bullet}$	triplet excited carbonyl
BSA	bovine serum albumin
CCD	charge-coupled device
DHE	dihydroethidium
DNP	2,4-dinitrophenylhydrazone
DNPH	2,4-dinitrophenylhydrazine
DTT	dithiothreitol
EPR	electron paramagnetic resonance
$FeSO_4 \cdot 7H_2O$	iron (II) sulfate heptahydrate
H_2O_2	hydrogen peroxide
HNE	4-hydroxy-2-nonenal
$HO^{\bullet}$	hydroxyl radical
HRP	horseradish peroxidase
MDA	malondialdehyde
O_2	molecular oxygen
$O_2^{\bullet-}$	superoxide anion radical
PDT	photodynamic therapy
$ROO^{\bullet}$	reactive peroxyl radical
ROS	reactive oxygen species
SDS	sodium dodecyl sulphate
TRIS	tris(hydroxymethyl)aminomethane
UPE	ultra-weak photon emission
UV	ultraviolet

8   Appendices

Published article (co-author) - the author contributed in data curation and participated in the drafting of the first version of the manuscript.

https://doi.org/10.3390/ijms24043981